Natural Environment Research Council

Institute of Geological Sciences

Mineral Reconnaissance Programme Report

A report prepared for the Department of Industry

D. Ostle
Programme Manager
Institute of Geological Sciences
154 Clerkenwell Road
London EC1R 5DU

No. 23

Disseminated sulphide mineralisation at Garbh Achadh, Argyllshire, Scotland

INSTITUTE OF GEOLOGICAL SCIENCES

Natural Environment Research Council

Mineral Reconnaissance Programme

Report No. 23

Disseminated sulphide mineralisation at Garbh Achadh, Argyllshire, Scotland

Geology and Geochemistry

R. A. Ellis, BSc, MIMM

Geophysics

G. R. Marsden BSc

Mineralogy

N. J. Fortey, BSc

London 1978

A report prepared for the Department of Industry

Mineral Reconnaissance Programme Reports

1 The concealed granite roof in south-west Cornwall

2 Geochemical and geophysical investigations around Garras Mine, near Truro, Cornwall

3 Molybdenite mineralisation in Precambrian rocks near Lairg, Scotland

4 Investigation of copper mineralisation at Vidlin, Shetland

5 Preliminary mineral reconnaissance of Central Wales

6 Report on geophysical surveys at Struy, Inverness-shire

7 Investigation of tungsten and other mineralisation associated with the Skiddaw Granite near Carrock Mine, Cumbria

8 Investigation of stratiform sulphide mineralisation in parts of central Perthshire

9 Investigation of disseminated copper mineralisation near Kimelford, Argyllshire, Scotland

10 Geophysical surveys around Talnotry mine, Kirkcudbrightshire, Scotland

11 A study of the space form of the Cornubian granite batholith and its application to detailed gravity surveys in Cornwall

12 Mineral investigations in the Teign Valley, Devon. Part 1—Barytes

13 Investigation of stratiform sulphide mineralisation at McPhun's Cairn, Argyllshire

14 Mineral investigations at Woodhall and Longlands in north Cumbria

15 Investigation of stratiform sulphide mineralisation at Meall Mor, South Knapdale, Argyll

16 Report on geophysical and geological surveys at Blackmount, Argyllshire

17 Lead, zinc and copper mineralisation in basal Carboniferous rocks at Westwater, south Scotland

18 A mineral reconnaissance survey of the Doon-Glenkens area, south-west Scotland

19 A reconnaissance geochemical drainage survey of the Criffel–Dalbeattie granodiorite complex and its environs

20 Geophysical field techniques for mineral exploration

21 A geochemical drainage survey of the Fleet granitic complex and its environs

22 Geochemical and geophysical investigations north-west of Llanrwst, North Wales

23 Disseminated sulphide mineralisation at Garbh Achadh, Argyllshire, Scotland

The Institute of Geological Sciences was formed by the incorporation of the Geological Survey of Great Britain and the Geological Museum with Overseas Geological Surveys and is a constituent body of the Natural Environment Research Council

Bibliographical reference
Ellis, R. A. and others. 1978. Disseminated sulphide mineralisation at Garbh Achadh, Argyllshire, Scotland *Miner. Reconnaissance Programme Rep. Inst. Geol. Sci.*, No. 23

Printed in England for the Institute of Geological Sciences by Ashford Press Ltd.

C O N T E N T S

LIST OF ILLUSTRATIONS

SUMMARY

A brief investigation of low-grade copper mineralisation associated with a small, calc-alkaline porphyry intrusion of Caledonian age is described.

Geological mapping has delineated a small stock of biotite-feldspar porphyry, 0.25 km^2 in area, intruded into a sequence of Dalradian schists and quartzites with inter-bedded epidiorites. Disseminated sulphides occur within the porphyry and the hornfelsed epidiorite but do not normally exceed 3% of the rock by volume. Assays of both rock types obtained maximum levels of 0.24% Cu. Hydrothermal alteration is prominent within the porphyry, with the widespread development of sericite and kaolinite. Subsequent faulting apparently exerted some control on the present limits of alteration and mineralisation. Several small strata-bound lenses of massive sulphide within the metasediments were recorded but were not investigated in detail.

Geochemical rock-sampling delineated a strong arcuate copper anomaly over the northern epidiorite/porphyry contact and a more subdued anomaly along the southern faulted contact. Molybdenum shows a similar distribution but is more closely confined to the porphyry. Overburden sampling demonstrated that little or no metal dispersion occurred within the overlying till, and stream sediment sampling of the catchment area showed that concentrations of copper decrease to background levels within 1 km of the intrusion.

Induced polarisation (IP) surveys produced a clearly defined grouping of chargeability anomalies around the edges of the porphyry stock but these showed no increase in magnitude at depth. Above background chargeability values recorded over the centre of the intrusion increase markedly towards the margins, possibly reflecting a pyritic halo. Most resistivity 'lows'

coincide with fault zones and the results of a total intensity magnetometer survey showed that, while most magnetic anomalies occur over epidiorites, significant anomalies are also produced in the vicinity of fault zones.

The results of the geological, petrographic, geochemical and geophysical studies demonstrate the presence of several features characteristic of 'porphyry copper style' mineralisation but the small surface area and low grade of the deposit, combined with a lack of encouraging geophysical responses at depth, suggest that there is little chance of discovering an economic orebody by exploratory drilling.

INTRODUCTION

In 1973-1974, Consolidated Gold Fields Limited undertook extensive geochemical and geophysical surveys in the vicinity of Garbh Achadh, Argyllshire. Results from this work and from outcrop mapping led the company to undertake a short programme of scout drilling. This survey indicated the presence of disseminated copper mineralisation. The Institute's interest in the area arose from a study of the company results and from a comparison with the Kimelford area, 15 km to the west, where porphyry style mineralisation is associated with a similar calc-alkaline porphyry intruded into low-grade Dalradian metamorphic rocks (Ellis et al., 1977).

As the detailed geochemical soil surveys completed by the company had already outlined the extent of surface mineralisation, only limited soil surveys were carried out in the present study, greater emphasis being placed on rock sampling. It was hoped that an attempt to delineate zones of hydrothermal alteration by surface mapping and petrographic studies, combined with deeper penetration geophysical surveys, might together provide evidence for the existence of more extensive mineralisation at depth. The work was undertaken in the spring and summer of 1976.

LOCATION AND GEOGRAPHICAL SETTING

Garbh Achadh is a rugged, upland area some 400 to 500 m above sea-level, straddling the watershed between Loch Fyne and Loch Awe in Argyllshire, Scotland (Fig. 1). It is situated approximately 6 km WNW of Inverary and access is either on foot from High Balantyre Farm (NN078118), or by forestry track from Eredine on Loch Awe (NM963084). The regional strike of the strata is to the north-east and has exerted the principal control on both the drainage and the topography. Except on the ridges where glacial scour has provided good exposure, glacial drift is widespread and there is an extensive

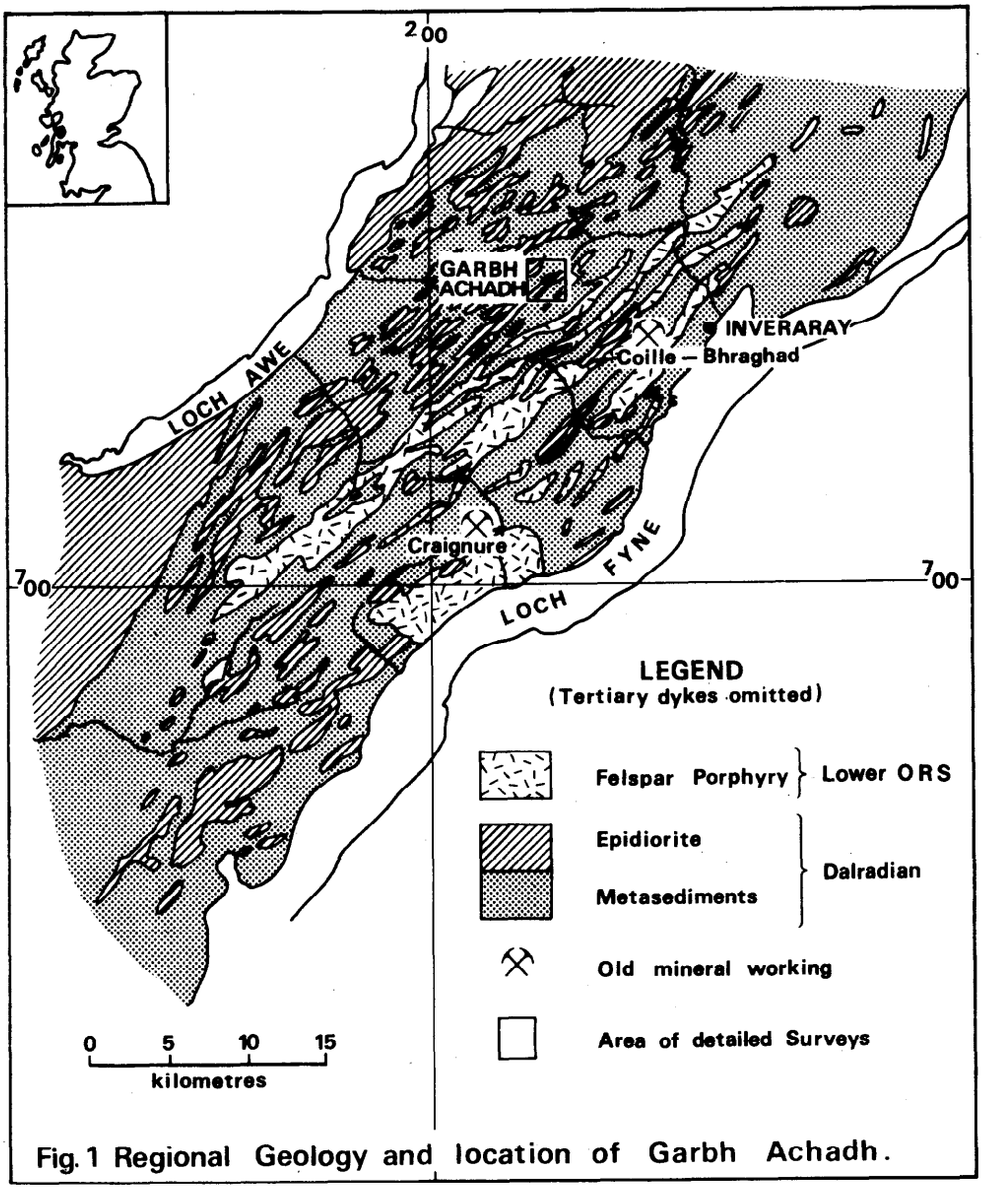

Fig. 1 Regional Geology and location of Garbh Achadh.

peat cover with large tracts of boggy and waterlogged ground and numerous small lochans.

Rough pasture on the summits of the hills affords a limited amount of sheep grazing and much of the lower ground is being drained in preparation for re-afforestation.

REGIONAL GEOLOGY

Between Loch Fyne and Loch Awe the regional geology comprises a sequence of Middle Dalradian (Lower Cambrian) metasedimentary and metabasic rocks which are intruded in the south-east of the area by a series of inclined quartz-feldspar porphyry sheets of Caledonian age (Fig. 1). These extend over a strike length of 24 km from Glen Shira in the north to the vicinity of Crarae on Loch Fyne in the south-west where the width of the belt is some 5 km. The combined thickness of the sheets is probably several thousands of metres. Whilst most of the sheets appear to be regionally concordant, at Garbh Achadh, located at the north-west limit of the belt, a small stock of feldspar porphyry is demonstrably discordant. It is characterised by a distinct thermal aureole and the development of hydrothermal alteration associated with low-grade disseminated copper mineralisation. The mineralisation extends into the adjacent Dalradian grits and epidiorites and is almost certainly controlled to some extent by faulting.

The Dalradian rocks are represented by a sequence of quartzites, quartz-schists and occasional pelitic horizons, which comprise the Crinan Sub-group of the Argyll Group, a part of the Dalradian Super Group (Harris and Pitcher, 1975). Interbedded with the Crinan Grits are a number of epidiorite sheets which represent metamorphosed basic sills and possibly some lava flows. The disposition of the Dalradian rocks in the South-West Highlands is mainly controlled by the effects of a primary Caledonian deformation. In the vicinity of Garbh Achadh the relatively steep stratigraphic dip of the Crinan Grits to the north-west reflects their geographical position midway between the axes of two major isoclinal structures formed by this early deformation,

the Loch Awe Syncline to the north-west and the Ardrishaig Anticline to the south-east. Subsequent Caledonian deformation produced more moderate folding and is reflected in a shallow dipping foliation superimposed on the earlier structures.

For a more detailed account of the regional geology, reference should be made to the 'The Grampian Highlands' - British Regional Geology Series (Johnstone, 1966) and to the Geological Survey Memoir of Mid-Argyll - Explanation to Sheet 37 (Hill and others, 1905). A detailed account of the Dalradian lithology has been given by Knill (1963) and, more recently, lucid accounts of the structure and stratigraphy of the Dalradian of the South-West Highlands have been given by Roberts (1974) and Roberts and Treagus (1977).

Previous mining activity within the district is limited to the two small mines at Craignure and Coille-bhraghad on the west side of Upper Loch Fyne near Inverary (Fig. 1) where small massive strata-bound sulphide deposits in quartz schists were worked briefly for copper and nickel in the last century (Wilson and Flett, 1921). Near Garbh Achadh, similar massive sulphide bands occur in thin quartzite beds but at a higher stratigraphic level. These may represent the lateral equivalents of a 'pyrite zone' which has been recognised in the Dalradian rocks of Perthshire, some 60 km to the north-east (Smith and others, 1977). The exact stratigraphic equivalents of the one or more sulphide-rich horizons are complicated, however, by the facies changes which occur both across and along the strike. Evidence of past interest in the strata-controlled deposits at Garbh Achadh is indicated by the presence there of a small trial and dressing-floor.

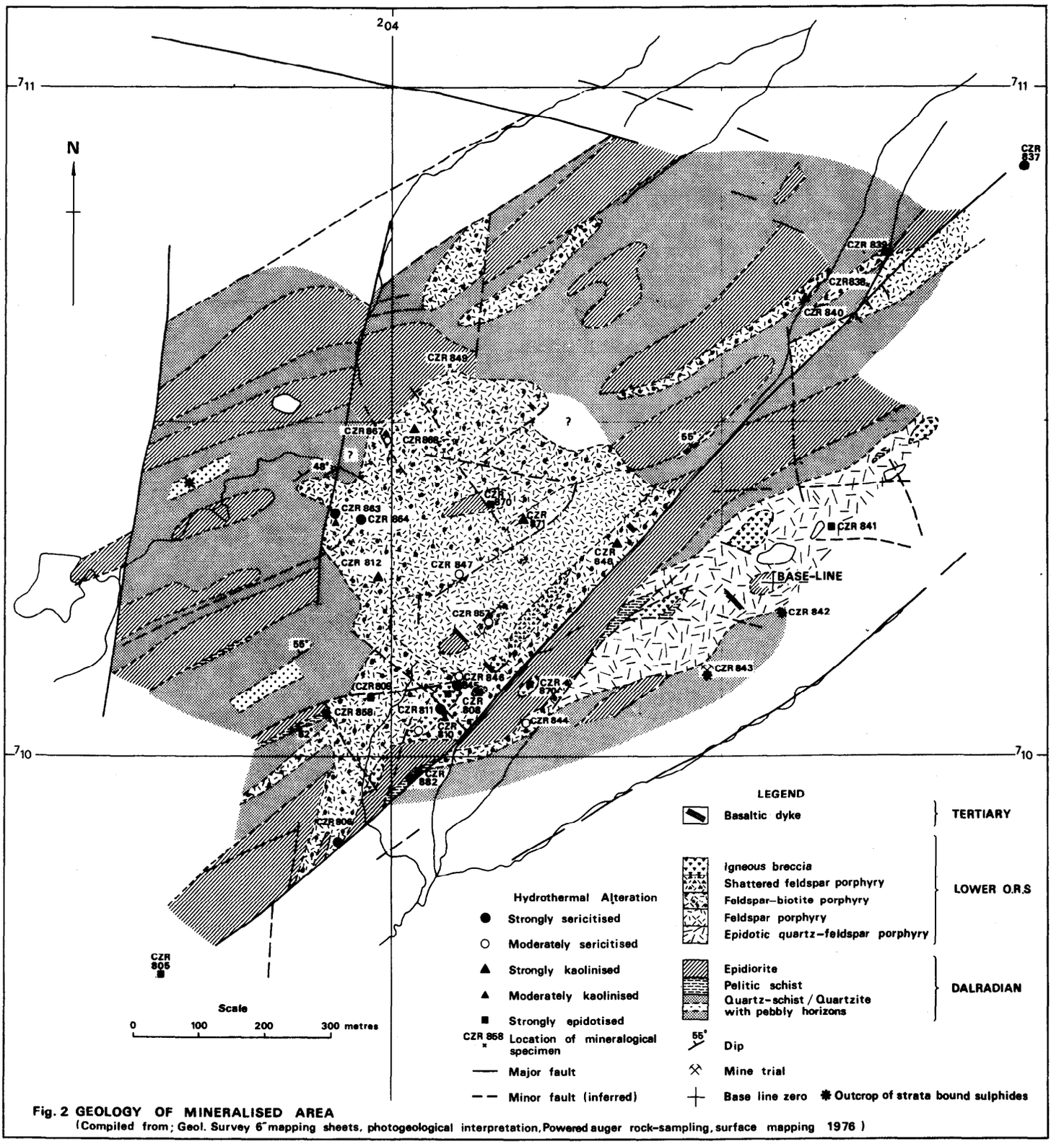

Fig. 2 GEOLOGY OF MINERALISED AREA

(Compiled from; Geol. Survey 6"mapping sheets, photogeological interpretation, Powered auger rock-sampling, surface mapping 1976)

GEOLOGY OF THE MINERALISED AREA

The geology of the mineralised area, presented in Fig. 2, is a compilation based on the original Geological Survey 6" sheets and rapid reconnaissance mapping supplemented by powered-auger rock sampling of the sub-drift outcrop and photogeological interpretation.

Photogeology

Air photographs on a scale of 1:10,000 are available from the Scottish Development Department, Edinburgh, and the following photographs provide full stereoscopic coverage: print nos. F/21/0414-0417, F22/0414-0417, from sortie no. 82/870. Garbh Achadh is located at the periphery of the photographs, where distortion is at a maximum.

A marked NE-SW sub-parallel alignment of the physical features is evident on the photographs and reflects the strong control of the regional Dalradian strike. At Garbh Achadh the small porphyry intrusion locally distorts the regional 'grain' and is discernible on the photographs as a pale-coloured positive feature indicating a thinner vegetation cover and possibly the bleaching effects of hydrothermal alteration. Within the contact aureole at Garbh Achadh, indurated epidiorites, quartzites and quartz schists locally form strong, positive, linear features.

Three major lineation directions are discernible on the photographs, at 010°, 040°, and 110°; they are believed to represent fault structures (Fig. 3). The 110° lineations occur to the north of Garbh Achadh and can be traced over several hundred metres to the WNW. The 040° lineations control the drainage pattern on the south-eastern limit of the intrusion and in the field at least one is demonstrably of faulted origin. On the western margin of the intrusion, two sub-parallel lineaments at 010° locally deflect the drainage pattern.

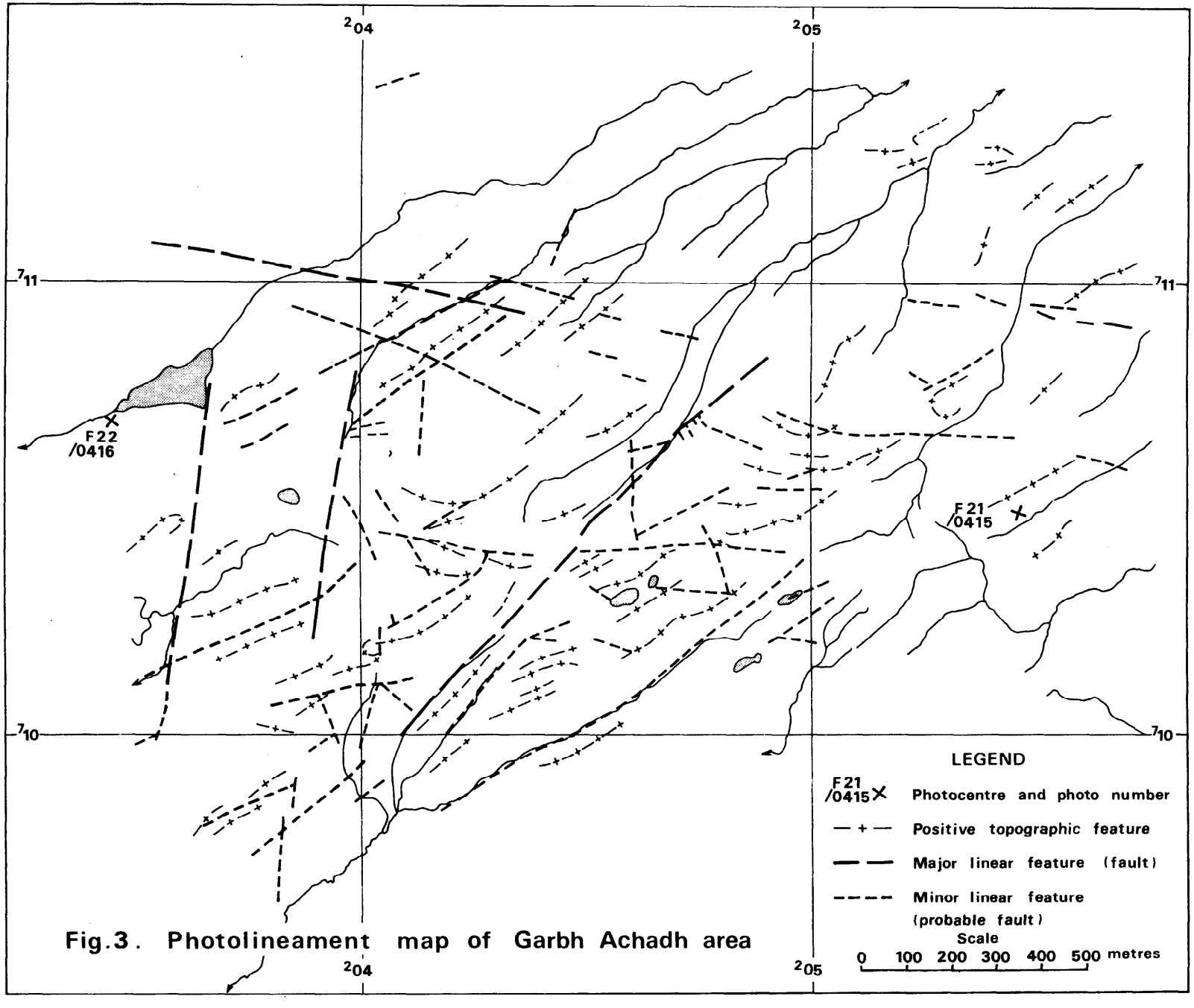

Fig.3. Photolineament map of Garbh Achadh area

The triangular configuration of the three sets of photolineations at Garbh Achadh, effectively enclose the intrusion and adjacent mineralised hornfels.

Several less conspicuous minor lineations can be detected with the aid of the stereoscope, aligned at approximately 060° and 145°. The 060° direction is parallel to the regional strike and lineaments in this direction probably represent either small strike faults or actual lithological contacts. The 145° direction coincides with the strike of the Tertiary dykes emanating from the Mull centre to the north-west. Two such dykes are exposed intermittently in the area, but the causes of most of the 145° lineations are obscured by drift.

Description of major rock types

Crinan Grits.

Within the area the Crinan Grits dip steeply to the north-west and comprise a sequence of buff/grey, fairly coarse, sometimes pebbly, quartzites and quartz-schists with occasional flaggy horizons. They are compositionally fairly pure although poorly sorted arkosic horizons rich in microcrystalline chlorite do occur together with thin, banded pelitic intercalations. Where exposed near the contact with the porphyry intrusion, the pelitic horizons are visibly hornfelsed, in contrast to the quartzite in which recrystallisation is not easily discernible in hand specimen. On the western contact, strongly banded metasediment adjacent to an epidiorite shows alteration of the pelitic horizons to actinolitic amphibole, epidote and quartz with the development of sericite and quartz veinlets in the intervening, more felsic laminae. Granular pyrite is developed in both assemblages and also as streaks in microfissures.

Epidiorites.

Epidiorites account for almost 50% of the country rocks in the vicinity of Garbh Achadh. They form relatively steep-dipping, tabular bodies concordant with the surrounding quartzites and often form prominent ridges. The larger bodies can be traced for several hundred metres along strike and their widths at outcrop frequently exceed 50m. In appearance the epidiorites are greenish-grey, medium to coarse grained melanocratic rocks weathering to dark brown at outcrop. They show pronounced foliation and flow-banding is common, particularly on their finer-grained margins. Although the lateral extent of contact metamorphism of the epidiorite is obscured to some extent by a regional albite-epidote facies of metamorphism, a progressive alteration of the epidiorites is apparent when traced towards the porphyry intrusion. At a distance of 300-400m from the porphyry, the epidiorites typically comprise hornblende (30%) and andesine plagioclase (55%) with minor epidote and granular iron oxide (CZR 805). Partial albitisation of the plagioclase, and slight sericitisation may be present associated with local developments of quartz, chlorite and epidote. Adjacent to the intrusion the epidiorites are markedly pyritised and hornfelsed and a specimen from the northern contact (CZR 849) shows a matrix of flow-banded plagioclase laths with sheaves of chlorite. No amphibole is apparent but epidote occurs throughout the rock both as minute grains and as coarse clusters associated with small patches and discontinuous veinlets of quartz.

Within the porphyry intrusion, two large rafts of epidiorite were mapped and a specimen from one of these (CZR 870), shows advanced alteration with much of the rock consisting of coarse clots of epidote in a matrix of chlorite. Also present are patches of mosaic-textured albite and sericite. Sulphides are present in only minor amounts but hematite is common.

Biotite-feldspar porphyry

The focus of the investigations at Garbh Achadh is a small intrusion of biotite-feldspar porphyry in which disseminated sulphides are associated with hydrothermal alteration. The intrusion is small in area ($0.25km^2$) and is truncated to the south by a north-east striking fault. Two small bodies, probably related at depth to the main intrusion, occur on the northern edge of the porphyry, and in the south-west the intrusion appears to be attenuated into one or two thin dykes. The intrusion is located on the north-western limit of a large group of feldspar porphyry sills in which sulphide mineralisation and hydrothermal alteration are generally not known to be significant. In the vicinity of Garbh Achadh, hydrothermal alteration of these sills is characterised by the development of epidote.

In thin section the main porphyry usually comprises some 30-50% sodic plagioclase phenocrysts showing various degrees of sericitisation in a fine felsic matrix in which small patches of quartz, some clearly of xenolithic origin, are generally present. The mafic constituents, biotite and hornblende, are generally replaced by chlorite and carbonate, pseudomorphs after the amphibole being distinguished by high carbonate contents, lack of a laminar structure and, in some cases, preservation of the characteristic form and cleavage of the basal prismatic section. Iron oxides and apatite are normally present in accessory amounts.

At outcrop the porphyry shows considerable variation in both colour and texture. It can vary from a rock in which feldspar phenocrysts are sparse and poorly developed to a porphyry in which large, euhedral phenocrysts of feldspar can account for almost 50% of the rock. Adjacent to large rafts of epidiorite the porphyry frequently has a chilled margin with the development of fine, granular texture and a lack of phenocrysts. Flow-banding is developed in the vicinity of bodies of igneous breccia.

The colour of the porphyry varies from dark-grey through various shades of buff and brown to a salmon-pink, epidotic variety in the vicinity of the brecciated rocks. The colour generally reflects the degree and type of hydrothermal alteration. Within the relatively unaltered, dark grey porphyry a high proportion of the feldspars are translucent and primary biotite is frequently retained. Where hydrothermal alteration is prominent the feldspar phenocrysts are opaque and the rock is more bleached in appearance.

The sporadic outcrops of dark grey biotite-feldspar porphyry are probably unaltered remnant patches within the intrusion. In some instances, however, they may represent post-mineralisation porphyry dykes. This is likely to be the case on the south-east margin of the porphyry where local outcrops of fresh grey porphyry occurring between the main fault and a parallel, linear zone of shattered porphyry are in marked contrast to the heavily altered nature of the porphyry in most other faulted areas.

Igneous breccia

Several outcrops of igneous breccia occur near the southern margin of the porphyry. They are generally lensoid in shape and range in width between 10 and 40m. In hand specimen, the rocks show a disordered fragmented texture in which epidote, pyrite and malachite are frequently conspicuous. Thin sections show that the larger fragments occur in a comminuted matrix of mineralogically similar material, and that many of the fragments show some degree of rounding. In most specimens the fragments appear to be of epidiorite or pelitic sediment rather than of porphyry but in one specimen (CZR 803) they consist entirely of porphyry and epidote-bearing plutonic rock. It is likely that the breccias represent rock fractured and (probably) fluidised during explosive gas releases, and could thus be described as tuffisitic breccia vent material.

These breccias show a propylitic type of alteration, the minerals formed including chlorite, epidote, calcite, sericite, pyrite, chalcopyrite and hematite. In some cases malachite and limonitic oxide phases represent limited supergene alteration.

MINERALISATION

A representative suite of 33 rock specimens was examined using petrographic thin sections, and the results of this work are summarised in Table I of Appendix II.

Two distinct types of sulphide mineralisation occur at Garbh Achadh; strata-bound, massive sulphides, similar in mode of occurrence to the exploited deposits at Craignure and Coille-bhraghad, and disseminated sulphides within the porphyry intrusion and adjacent hornfelsed epidiorite.

Within the biotite-feldspar porphyry, sulphide, predominantly pyrite, is disseminated throughout but rarely exceeds 3% of the rock. It is associated with a pervasive hydrothermal alteration in which sericite, muscovite and calcite form the most common secondary assemblage. Adjacent to small quartz veins the porphyry sometimes shows metasomatic alteration to a coarse orthoclase/quartz assemblage (CZR 863).

In some rocks kaolinite has developed by the replacement of plagioclase and coexists with sericite, muscovite and calcite. Where kaolinite is the dominant secondary phase primary biotite phenocrysts are generally preserved. The kaolinisation, or argillic alteration, is locally intense and is generally associated with an increase in the incidence of quartz veinlets. This is particularly evident towards the northern margin of the intrusion where,in addition, chalcopyrite in significant amounts, rare covellite, and minor molybdenite are present. Immediately adjacent to the contact supergene malachite sometimes occurs in small dilational quartz veins (CZR 863).

Although it is probable that the emplacement of the intrusion resulted in some redistribution and introduction of sulphides from the adjacent epidiorites and mineralised horizons within the metasediments, the restriction of molybdenite to the intrusion suggests that the molybdenum and probably much of the copper associated with the hydrothermal alteration is of magmatic origin.

Much of the sulphide adjacent to faults has been limonitised and distributed along numerous small hair fractures, and in some places the clay mineral illite is developed within the feldspars (CZR 806). Near the south-west faulted limit of the intrusion schlieren-like pockets of pyrite with minor chalcopyrite and molybdenite have been noted in thin-sections. At outcrop, where faulting is obvious, large (>1 cm) pyritohedra are commonly developed in cavities and small brecciated zones together with minor amounts of chalcopyrite and clay minerals.

Mineralisation associated with the igneous breccias is patchy and predominantly pyrite. Qualitative XRF has detected only minor amounts of Cu but significant levels of Ba (CZR 807).

Near the southern margin of the intrusion a raft of hornfelsed quartzite shows altered arkosic material in which sericite, chlorite, epidote and granular iron oxide are developed. Sulphides, predominantly pyrite with minor chalcopyrite, molybdenite, covellite and sphalerite, amount to almost 12% of this rock and are developed preferentially along small fractures (CZR 808). Similar mineralisation has not been recorded in the quartzites within the contact aureole.

Within the hornfelsed epidiorites adjacent to their contact with the porphyry intrusion, sulphides, principally pyrite with minor chalcopyrite and a trace of pyrrhotite locally approach 10% of the rock. They occur in disseminated form throughout but more particularly in silicified zones as

aggregates in small quartz veinlets. Elsewhere within the contact aureole, the overall sulphide content of the epidiorite rarely exceeds 1-2 per cent. Assay results from samples of both epidiorite and porphyry have provided maximum levels of 0.24% Cu.

The strata-bound sulphides are confined to thin quartzitic horizons (<1m in thickness) within the Crinan Grits and in the southern part of the area have been exploited in a small trial (NM 0447/1009). At this locality mineralisation varies in intensity from sparsely disseminated interstitial ore grains to wholesale massive replacement by sulphides. Pyrrhotite forms the bulk of the massive ore and pyrite and chalcopyrite are patchily distributed throughout. A level of 0.7% Cu was estimated (XRF) in one specimen (CZR 843).

Approximately 1700 m along strike to the north-east, a small dressing-floor has provided several specimens of massive sulphides formed at the junction of vein quartz with interbanded mica schist and micaceous quartzite. In one specimen (CZR 831) cleavage crenulations in the host schist continue into a development of massive ore. The sulphides are predominantly pyrite and chalcopyrite with lesser amounts of pyrrhotite. In one thin section (PTS 2406) a minor development of arsenopyrite and sphalerite is apparent on the margins of the chalcopyrite. Qualitative XRF located high levels of Cu and Ni and significant amounts of Zn, As and Co with traces of Cd, Ba and Ag,and quantitative levels of 13.2% Cu and 0.74% Ni were obtained from one specimen. The source of this material could not be located at outcrop but is presumed to be of local origin.

Although locally rich in copper, the limited thickness of these deposits and their restriction to one or two distinct horizons has not justified any detailed investigation and more significance is attached to the disseminated mineralisation associated with the porphyry intrusion.

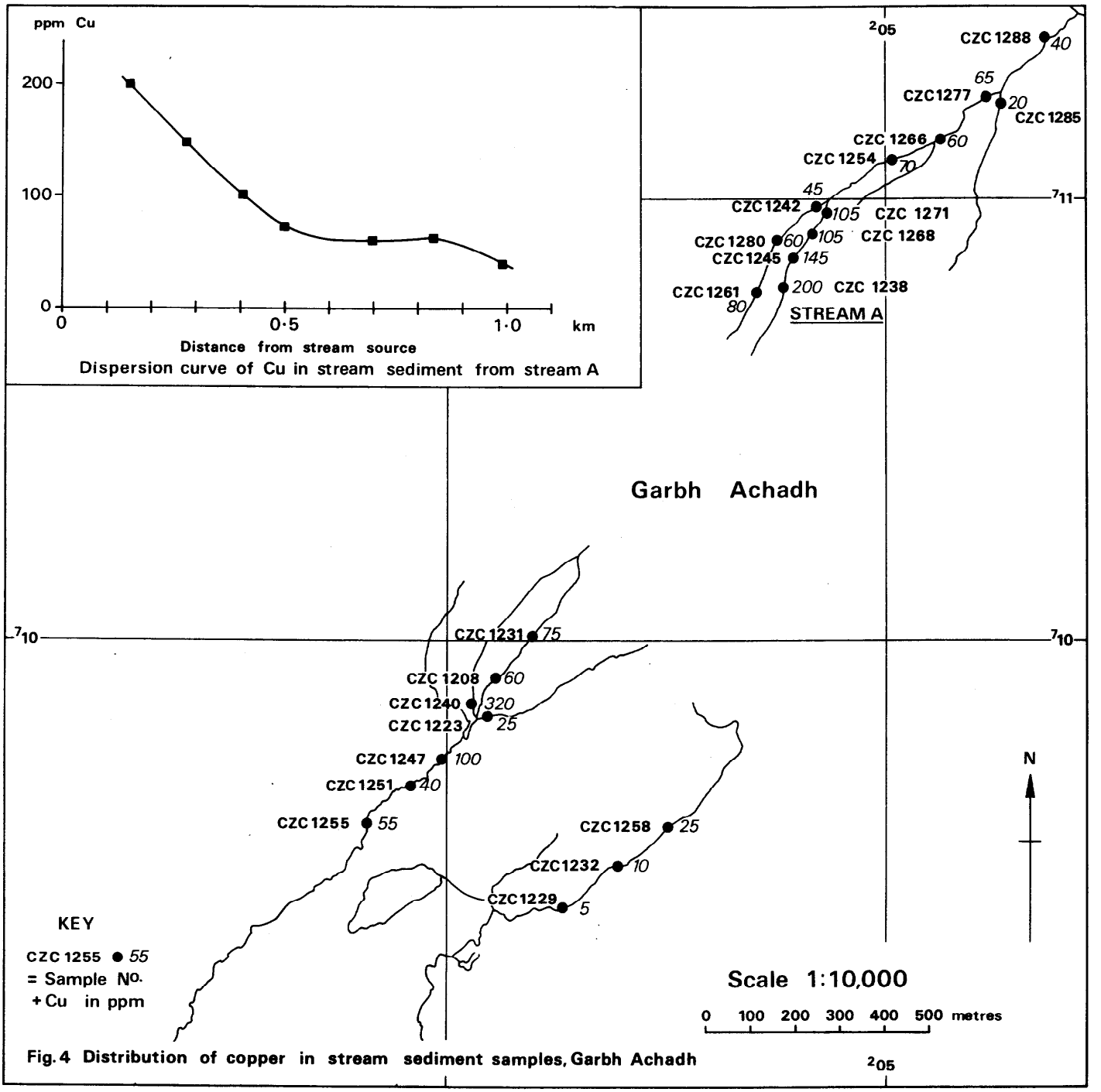

Fig. 4 Distribution of copper in stream sediment samples, Garbh Achadh

GEOCHEMISTRY

Stream sediment sampling

Three streams draining Garbh Achadh were selected for close interval sediment sampling and the results are presented in Fig. 4. The samples were wet sieved to -100 mesh in the field and were analysed for Cu, Ni, and Zn by atomic absorption spectrophotometry (A.A.S.).

The dispersion of copper in sediments from the stream draining to the north-east is displayed graphically as an inset in Fig. 4. Levels of copper are highly anomalous near the source (200 ppm Cu) but decrease gradually to background concentrations ($<$50 ppm Cu) over a distance of 1 km downstream. The smooth dispersion curve obtained from this stream is not repeated for the streams to the south-west. In the former stream, disseminated sulphides in the porphyry form a large dispersed source about the headwaters whereas in the south-western stream catchment area both disseminated sulphides and massive bedded sulphides contribute to the copper anomaly and have consequently produced a more variable dispersion pattern.

No strongly anomalous levels of nickel or zinc were found. Maximum concentrations were 165 ppm Ni and 460 ppm Zn, but some secondary concentration of the zinc is suspected.

Stream sediment sampling at Garbh Achadh indicates that the sample interval used in the Institute's regional drainage survey of the Dalradian area of western Scotland, (Tandy, in preparation), is of sufficient sample density to locate areas of similar mineralisation. This latter survey has shown that elsewhere in the region stream sediment samples derived from catchments underlain by non-mineralised porphyry provide levels of copper within the range 0-20 ppm.

Overburden sampling

Since extensive geochemical soil sampling had been carried out by Consolidated Gold Fields Limited, overburden sampling was limited to two traverses of profile-sampling across the central area at Garbh Achadh. The positions of these traverses were guided by the previous soil results. The objective was to establish the amount of dispersion in the secondary environment by comparison of the results with the attendant rock sampling.

Within the area investigated the overburden typically comprises one to two metres of peat underlain by a similar thickness of glacial till. Occasionally the peat cover exceeds four metres but this is exceptional. A total of 58 samples was collected, using a powered auger where necessary, and in most instances a sample of the basal till was collected together with a sample of the overlying peat. All samples were analysed for Cu, Pb, Zn and Ag (A.A.S.), and the results and sample details form Appendix I, parts 1 and 2B.

Anomalous levels of copper in basal till, generally in the range 200-700 ppm, were located over both the biotite feldspar porphyry and the adjacent hornfelsed epidiorite, with maximum concentrations of 2000 ppm Cu and 1500 ppm Cu respectively. The results also indicate a decrease to background levels ($<$ 50 ppm Cu), within 200-300 m of the porphyry/epidiorite contact, corresponding to a similar diminution in metal concentrations in rock samples from the same area. This suggests that dispersion within the drift was minimal.

The levels of lead, zinc and silver in basal till were nowhere found to exceed regional background concentrations and provided ranges of 10-50 ppm Pb, 10-90 ppm Zn, 1-2 ppm Ag.

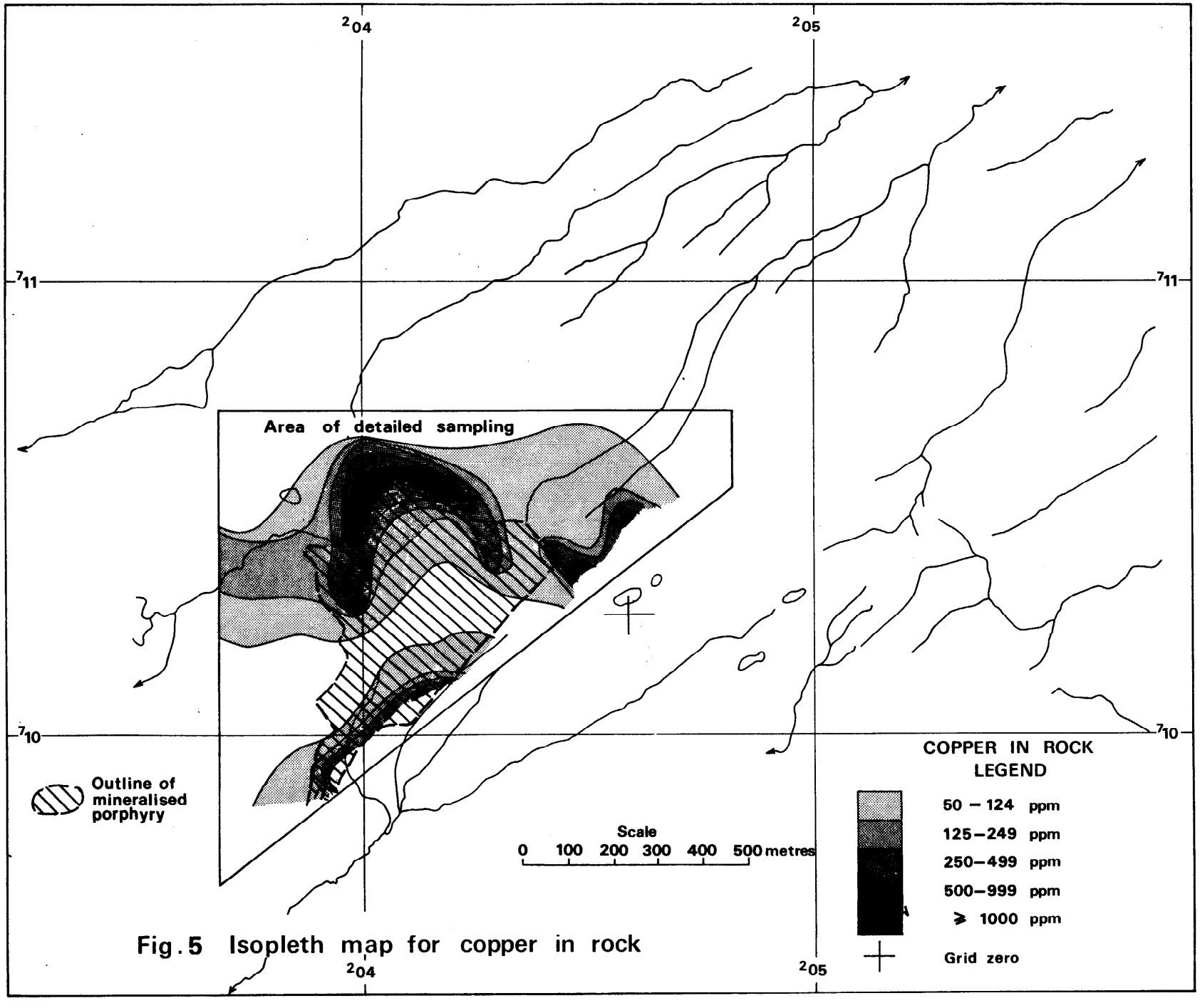

Fig. 5 Isopleth map for copper in rock

Similar ranges for lead, zinc and silver were obtained from the peat samples. Copper concentrations in peat showed considerable variation, but were generally appreciably lower than the corresponding till samples.

Rock sampling

Over the area of the porphyry intrusion and the adjacent metamorphic aureole, rock samples were collected on a 100 m grid. The grid was surveyed by compass and tape and the zero reference point is located at national grid reference NN 0458 1026. Where possible, samples were obtained as chips from outcrops but in areas of poor exposure samples were obtained from the sub-outcrop using the powered auger. The samples were analysed for Cu, Pb, Zn, Ag, Co, and Ni by A.A.S. and for Mo by X-ray fluorescence spectrometry. The results and location details are presented as Appendix I, parts 1 and 2 C, and isopleth maps for copper and molybdenum are depicted in Figs. 5 and 6.

The regional background level for copper in the Dalradian rocks of the district ranges between 5 and 50 ppm, with background levels in Caledonian calc-alkaline intrusives appreciably lower - generally in the range 3-20 ppm.

At Garbh Achadh anomalous copper concentrations fall into two zones, a linear anomaly (open to the south), along the southern faulted contact of the porphyry and a second broader zone running east-west across the northern limit of the intrusion and the adjacent country rocks. The southern anomaly can be attributed to thin sulphide-rich horizons in quartzite and to disseminated copper sulphides observed in a small zone of igneous breccia on the southern margin of the porphyry. Within the northern anomaly a strong arcuate zone of high copper (< 250 ppm), is broadly coincident with the northern margin of the intrusion and adjacent hornfelsed epidiorite. The peak value within this zone obtained from a sample of biotite-feldspar

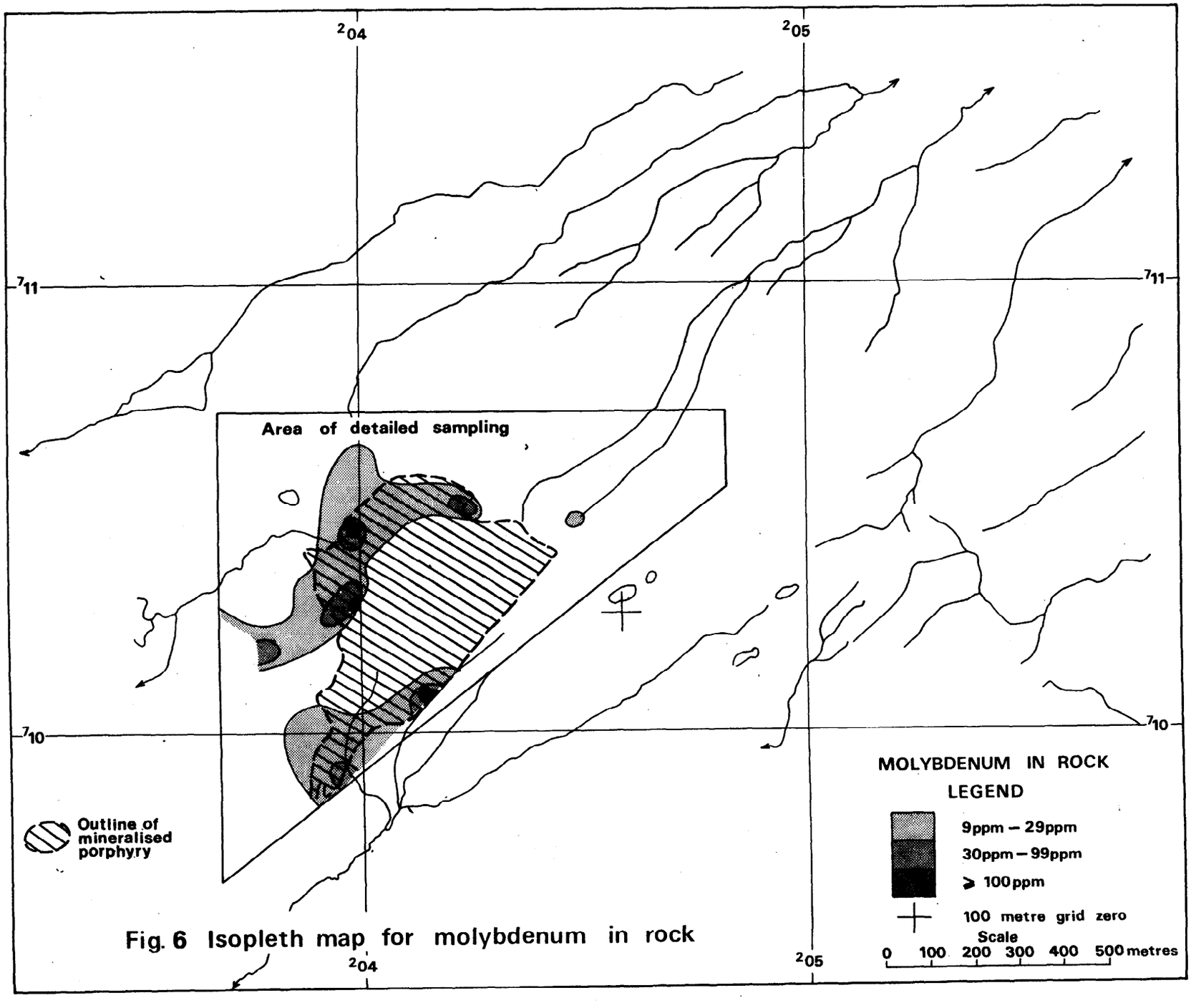

Fig. 6 Isopleth map for molybdenum in rock

porphyry was 0.24% Cu. The western limit of the arcuate zone appears to be controlled by a prominent NNE fault. To the east of the main anomaly a smaller, highly anomalous zone (open to the south-east), is related to an epidiorite adjacent to the north-east extension of the major fault which truncates the intrusion to the south-east.

Anomalous molybdenum concentrations in rock (Fig. 6) generally show a distribution similar to that of high copper values, but are more sharply confined to the limits of the porphyry intrusion. Concentrations range between 10 and 40 ppm Mo, with two high values of 574 ppm and 600 ppm Mo obtained from samples from the western margin of the porphyry. High concentrations of molybdenum within the porphyry are confined to areas where hydrothermal alteration is more intense and where kaolinisation and quartz veining are most prominent.

Concentrations of Pb, Zn, Co and Ni in rock are generally low, apart from one or two samples with slightly enhanced Co and Ni. Two samples, one of non-biotitic porphyry, the other of pelite, provided anomalous levels of Ag of 6 and 5 ppm respectively. The pelite sample also provided a level of 1075 ppm Cu. No great significance was read into either result.

The range of values for Pb, Zn, Ag, Co and Ni in rock together with their median values are as follows:-

Metal	Range	Median value
Pb	10 - 30 ppm	10 ppm
Zn	5 - 240 ppm	20 ppm
Ag	0.5 - 6 ppm	1 ppm
Co	2.5 - 85 ppm	10 ppm
Ni	2.5 - 140 ppm	20 ppm

GEOPHYSICAL SURVEYS

Introduction

During 3 weeks in July 1976 an induced polarisation (IP) and total intensity magnetic field survey was undertaken at Garbh Achadh. The work arose from recommendations by RMMU (Michie et al., 1975) for further examination of the IP anomalies which had been located in previous mining company exploration. In particular, the aims of the geophysical survey were to increase the depth of the IP observations and to determine the spatial relationship of these anomalies with the igneous bodies present at Garbh Achadh. By this means it was proposed to examine the hypothesis that the mineralisation at Garbh Achadh was of a 'porphyry' copper style and that the recorded IP anomalies were due to an associated pyritic halo.

Measurements

The survey, centred over the small pyritiferous, biotite feldspar porphyry body, was conducted along 7 north-south traverses at 200 m intervals and 3 east-west cross-lines at intervals of 420 metres; the central cross-line corresponded to the geochemical survey baseline (Fig. 7). Induced polarisation observations were recorded along all traverses using time domain HUNTEC MkIII IP equipment in a 'dipole-dipole' configuration. A dipole length (a) of 60 metres was used throughout, with dipole spacings of 120 m to 360 m (i.e. n=2 to 6 measured between dipole centres). On one occasion (along part of Line 600W) a larger dipole length of 120 metres was employed. Total field magnetic intensity observations were recorded along all north-south traverses using an ELSEC nuclear precession magnetometer. In total, the main phase of the IP survey covered a distance of 13.4 line kilometres, while the greater penetration (120 metre dipoles) coverage was restricted to 0.8 line kilometres.

Presentation of results

All the magnetic results are presented as profiles superimposed over a map showing the principal geological elements (Fig. 8). The IP chargeability and resistivity results for n=2 are presented as contours on the same geological base map (Figs. 9, 11). The chargeability and resistivity results for n=6 are presented as contour maps (Figs. 10, 12). In addition the IP results are presented in full as two dimensional vertical pseudo-sections for each traverse together with magnetic profiles (Appendix III, Figs. A3.1-11).

Discussion of results

Magnetic survey

A comparison of the magnetic field values with the exposed surface geology suggests that both the non-biotitic feldspar porphyry and the main pyritiferous feldspar porphyry are associated in general with a quiet background level (approx. 49,000 nT). The magnetic response over the epidiorite is variable. Lines 200E, 00 and 200W for example show distinct positive or negative anomalies over exposed epidiorite whereas near the northern extremities of lines 200W, 400W and 800W, epidiorite has no anomaly. Over the metasediments the magnetic values tend to be about background level although distinct anomalies are recorded. These, however, are believed to represent an extension along strike of nearby sub-outcropping epidiorite.

The largest and most persistent magnetic anomalies occur close to the north-west and south-west margins of the main porphyry body. These anomalies, which straddle the boundaries drawn on the geological map for epidiorite and metasediment rocks, are in contrast to those anomalies over epidiorite in the east of the survey area, since there the extent of the anomaly is confined to the epidiorite alone. This contrast in response is possibly attributable to the

presence of pyrrhotite in the hornfelsed country rocks on the north-western margin of the main intrusion. Pyrrhotite is recorded within the hornfels there on the old six inch map of the Geological Survey and, in the course of the recent mapping, pyrrhotite was recorded in hornfelsed epidiorite on the northern margin of the intrusion at 500W/320N. Late-stage pyrrhotite forms the bulk of the replacement sulphide in a specimen of quartzite from position 100W/120S.

The large magnetic anomalies centred on line 600W at 350N and line 800W at 270N are almost certainly related to the pyrrhotite within the hornfelsed epidiorite. Taken together at this magnetic latitude, the shape of these anomalies suggests a line of shallow magnetic dipoles of limited depth dipping to the north-west. This association of thermally altered rocks with magnetic anomalies suggests that the magnetic response observed over the rocks at Garbh Achadh is related to their individual thermal histories. In particular, the magnetic properties of the Dalradian rocks around Garbh Achadh will have been largely determined by the degree of thermal metamorphism (and accompanying mineralogical changes) occurring in Caledonian times during the emplacement of the main porphyry body.

Induced polarisation

Inspection of all the chargeability data shows that values range between 1 and 123 ms with an average value of 35 ms ('m') and r.m.s deviation of 17 ms ('d'). In choosing a background level, it has been found convenient to adopt a value of approximately 18 ms (m - d) and to regard as anomalous, values exceeding 52 ms (m + d). Apparent resistivity values range from 300 to 7000 ohm metres. Low resistivity anomalies are only rarely associated with chargeability anomalies, being usually coincident with geological fault zones.

Varying resistivity values are in part due to the rugged topography encountered at Garbh Achadh, which inevitably distorts the resistivity contour patterns.

(a) Chargeability contours. A contoured plan of chargeability values (superimposed upon a geological background) at the shallowest level of investigation (i.e. n=2, Fig. 9), confirms the distribution and intensity of anomalous zones previously indicated by mining company investigations. Anomalies have been labelled A through to G. Relating the position of these anomalies to the known surface geology reveals that the largest anomalies (A-D) are centred over epidiorites and all fall within the thermal aureole of the biotite-feldspar porphyry intrusion. They are all associated with magnetic anomalies. No significant magnetic anomalies have been recorded over the smaller anomalies E, F and G. Over the main porphyry body, chargeability values are higher than background but do not attain anomalous levels. Two notable anomaly lows do however, straddle the margin separating metasediment from the main porphyry body. The weakly pyritiferous non-biotitic feldspar porphyry is associated with a chargeability low. At the maximum investigation depth (n=6, Fig. 10), numerous local anomalies are evident with the largest and most extensive still clustering about the margin of the main porphyry body. However, overall there is a recognisable ENE-WSW trend. Once again, for the main porphyry body values are above background but not anomalous.

(b) Apparent resistivity plan contours. Contouring apparent resistivity values for n=2, (Fig. 11), results in a pattern largely unrelated to that of the chargeabilities. The prominent north-east to south-west trending fault is clearly associated with a linear string of resistivity lows. Other faults, striking nearly parallel with the survey traverse lines have

generally not been detected. Of the chargeability anomalies, only A and D are associated with significant resistivity lows. The broad zone of low resistivity in the south-west of the area is associated with an equally broad string of magnetic anomalies which together are believed to be related to the nearby parallel fault. An elongate resistivity high, centred over the main porphyry body, extends to the south-west over metasediment. Other highs occur over metasediment in the west and weakly pyritiferous feldspar porphyry in the east. At depth n=6, (Fig. 12), the resistivity highs over the main porphyry body and weakly pyritiferous porphyry persist. Furthermore the numerous resistivity lows display a distinct ESE-WNW trend.

(c) Pseudo-sections. These are presented and described in detail in Appendix III

Assessment of results

In assessing all the geophysical results available for the Garbh Achadh prospect, the following summary of observations emerge.

(i) The present IP survey has confirmed the distribution and intensity of IP gradient array anomalies originally detailed during mining company investigations. These anomalies have been labelled A through to G (Fig. 9).

(ii) Superimposed upon a general north-east to south-west trend, the dominant near surface (n=2) chargeability anomalies exhibit a tendency to cluster about the edge of the main biotite-feldspar porphyry body. At depth, the anomalies develop a more pronounced east-west trend.

(iii) These chargeability anomalies (A to E incl.) usually correspond with exposed epidiorite containing sulphides, in particular with those parts of the epidiorites subjected either to thermal alteration during emplacement of the main porphyry intrusion or to later episodes of faulting. Furthermore,

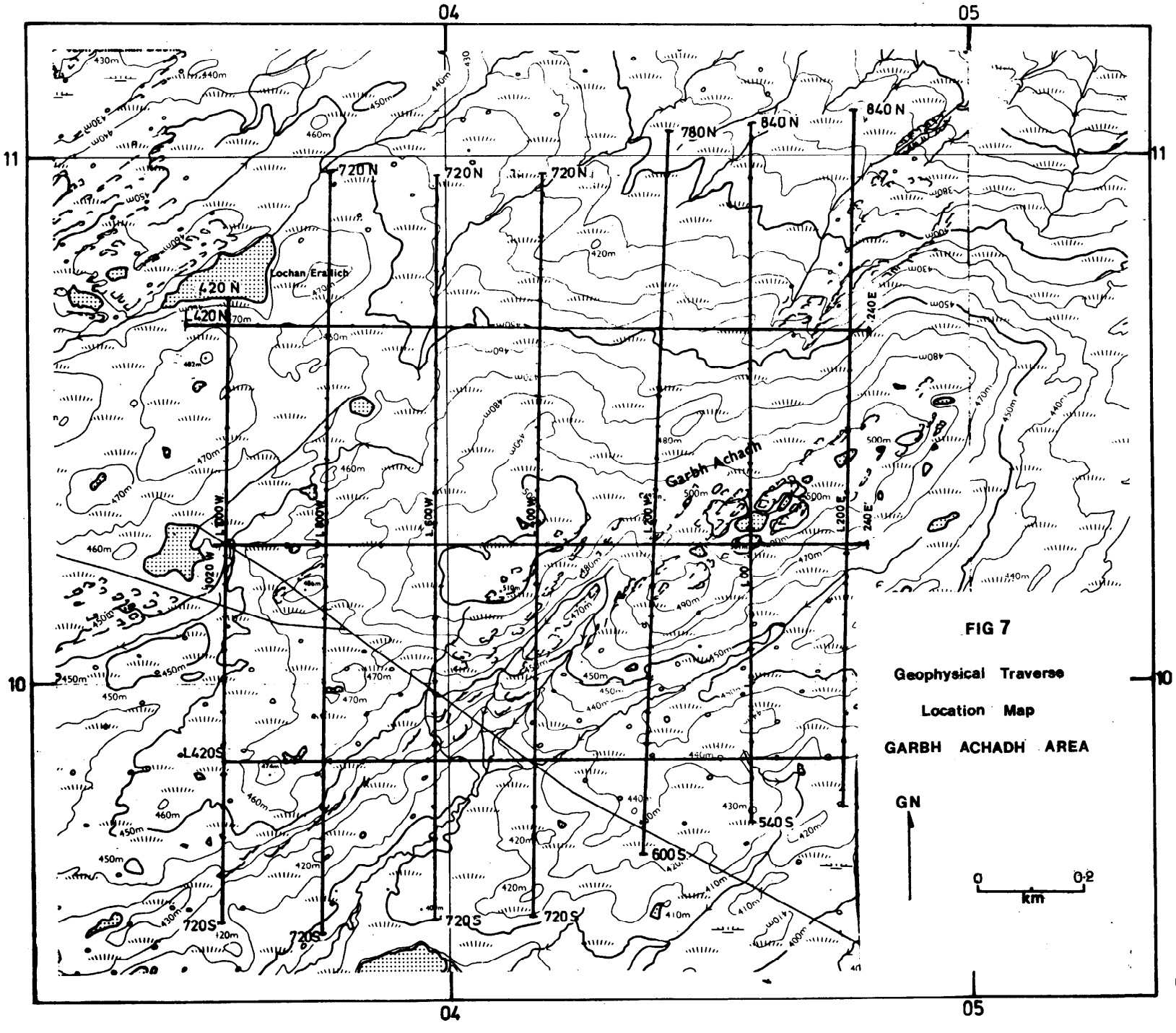

FIG 7

Geophysical Traverse

Location Map

GARBH ACHADH AREA

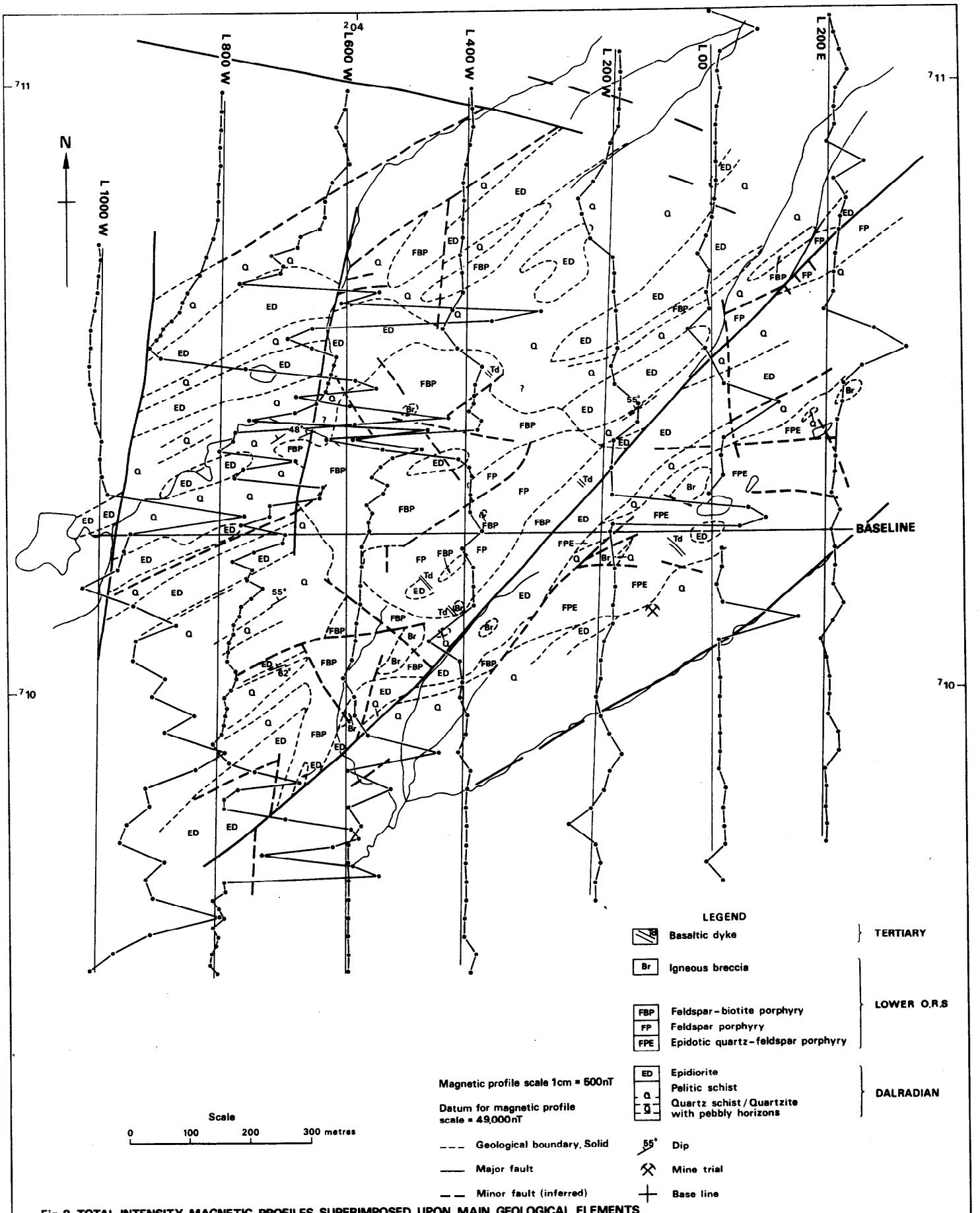

Fig. 8 TOTAL INTENSITY MAGNETIC PROFILES SUPERIMPOSED UPON MAIN GEOLOGICAL ELEMENTS

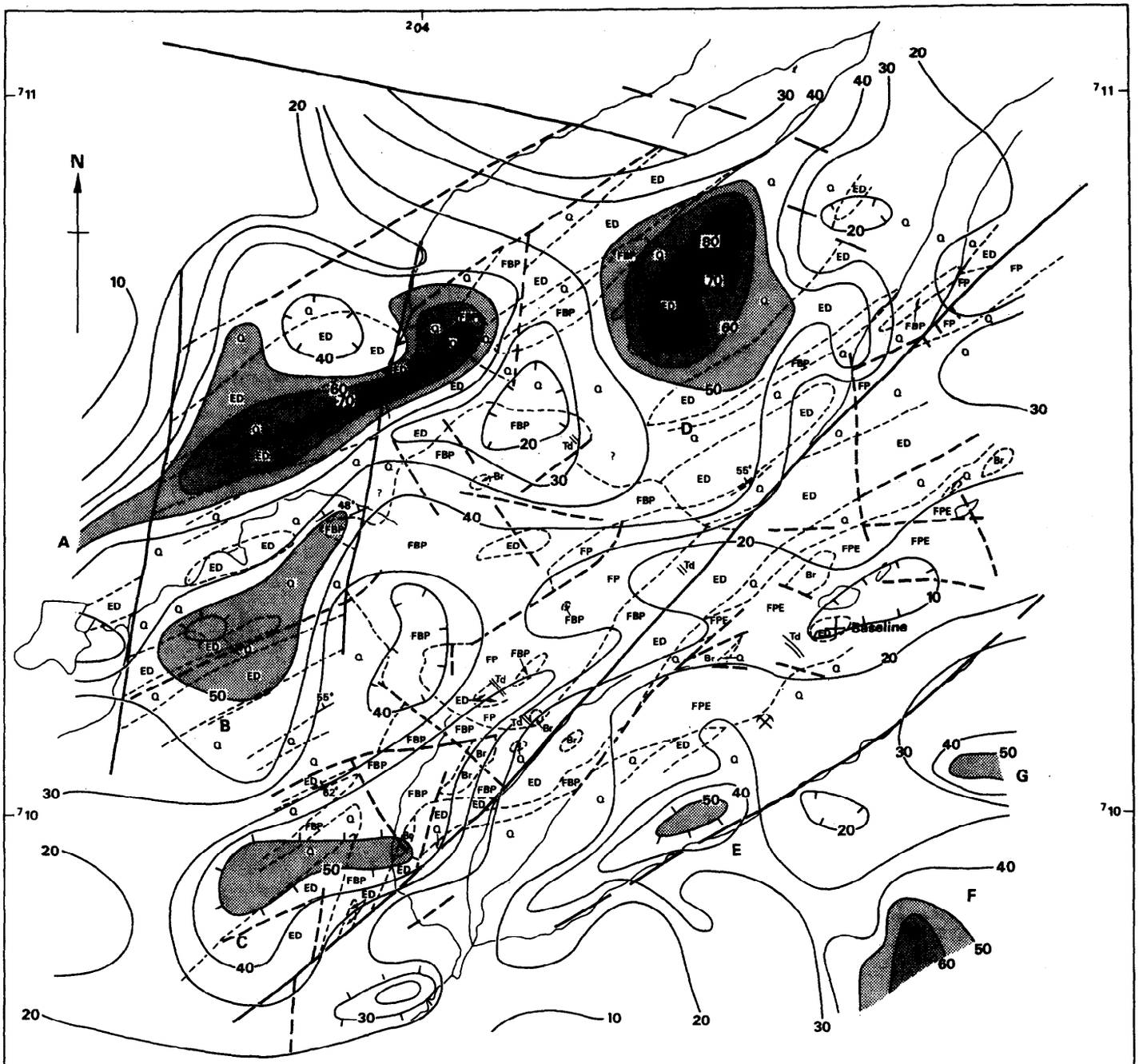

Fig.9 CHARGEABILITY CONTOURS, N·2

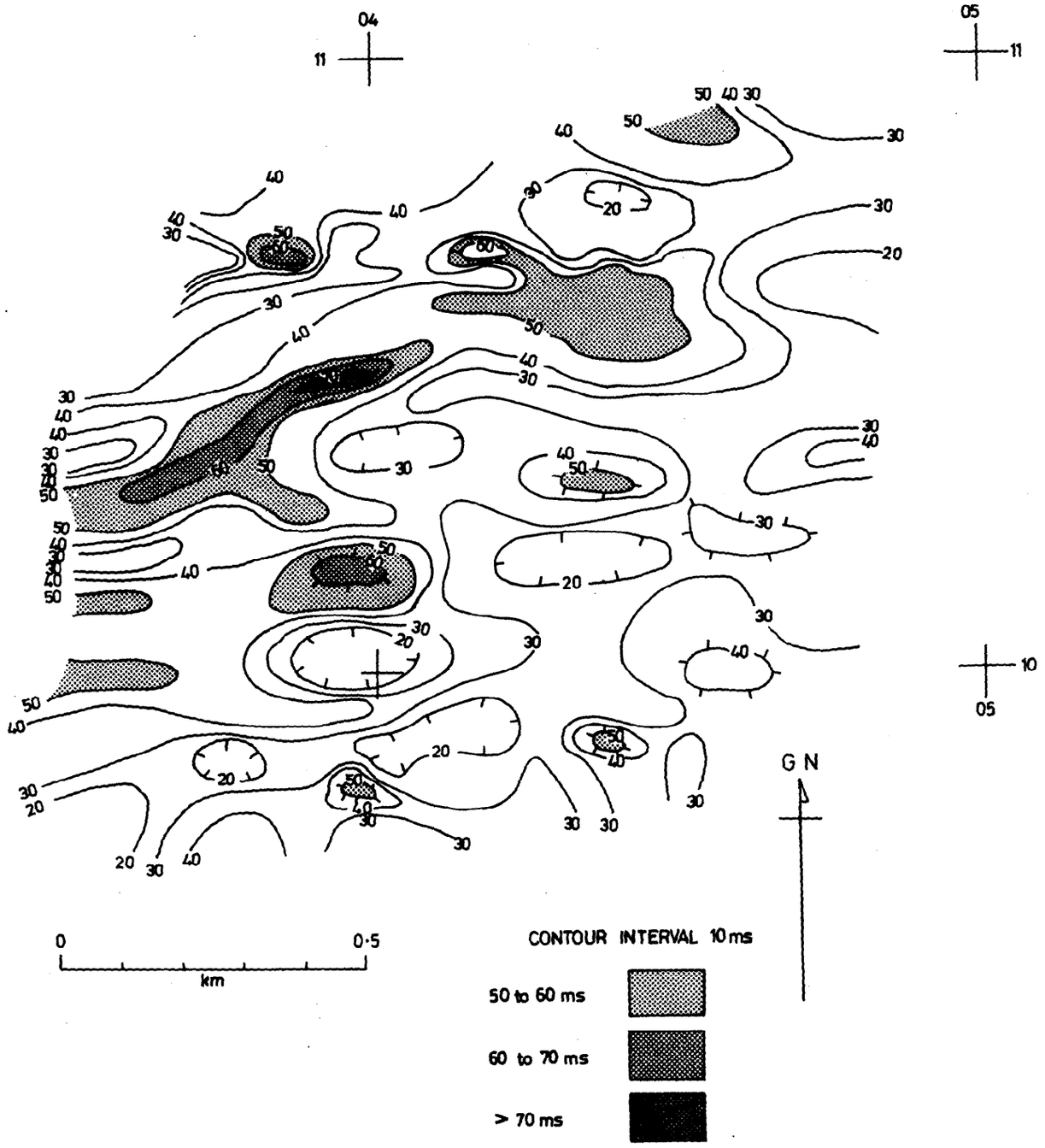

Fig. 10 IP CHARGEABILITY CONTOURS FOR N = 6

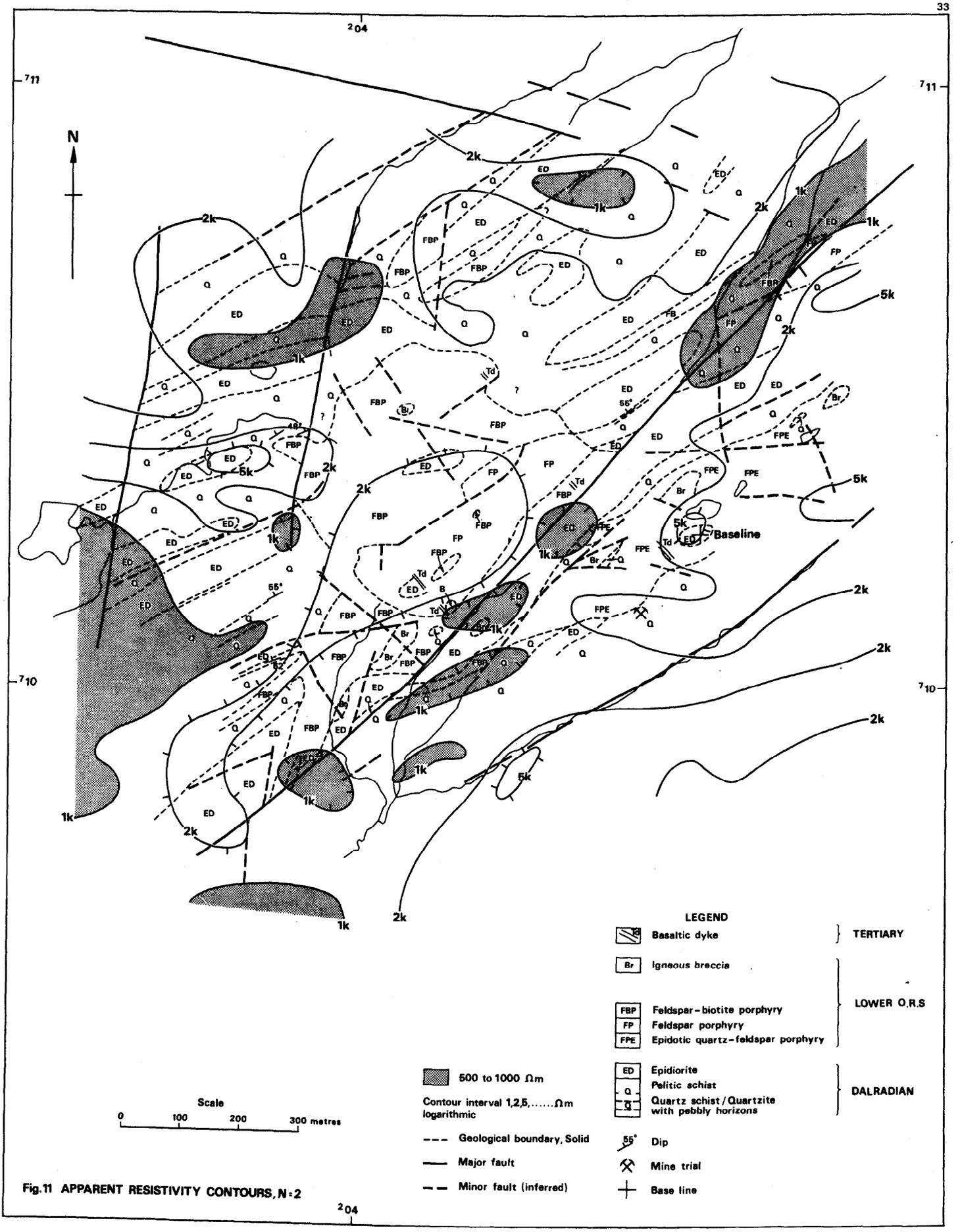

Fig.11 APPARENT RESISTIVITY CONTOURS, N=2

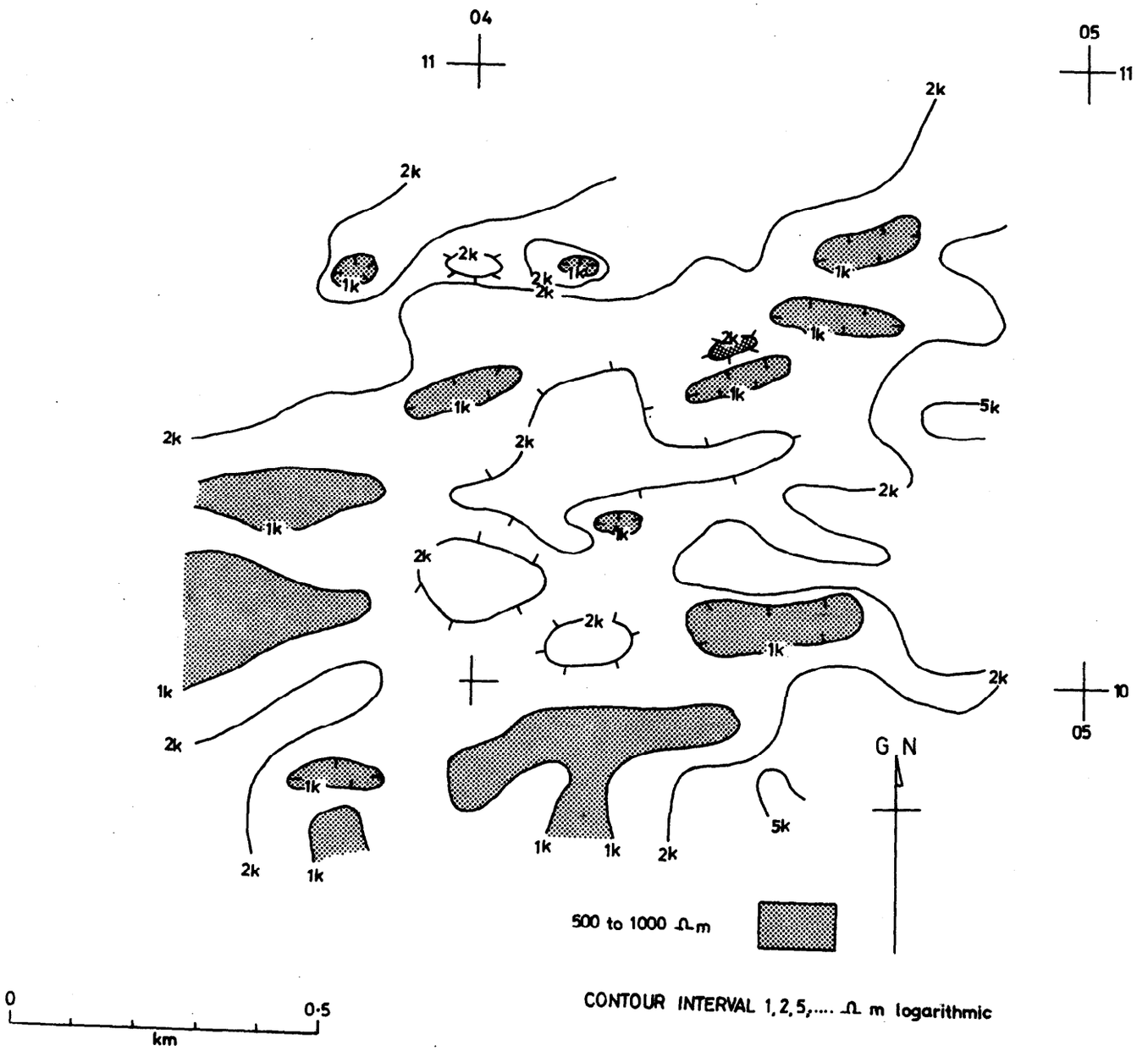

Fig.12 APPARENT RESISTIVITY CONTOURS FOR N = 6

it is evident that post-intrusion faulting has been effective in disrupting any originally imposed IP chargeability pattern circumscribing the main porphyry body.

(iv) All the major IP anomalies (A,B,C and D) extending to n=6 on the vertical pseudo-sections are associated with similar chargeability patterns, each of which suggest (by comparison with IP scale models) that the anomalous source is of a shallow (typically 60 m deep) 'slab-like' zone of disseminated mineralization. Follow-up deeper penetration work (120 m dipoles) also indicates that the sources responsible for the IP anomalies probably neither widen nor continue significantly at depth.

(v) Except for anomalies A and D, apparent resistivity lows do not coincide with chargeability highs, being more often associated with fault zones.

(vi) Magnetic anomalies, whilst not exclusively associated with epidiorite, do occur without exception over those epidiorites nearest to the margin of the main biotite-feldspar porphyry body. Furthermore, both epidiorite and the metasediments display magnetic anomalies close to fault zones.

Interpretation

The geophysical results obtained from this survey show both affinities with, and departures from, those which one would expect for the model proposed by Lowell and Guilbert (1970) for a typical porphyry copper deposit.

At Coed-y-Brenin in North Wales a small porphyry copper deposit of probably earlier age than the Garbh Achadh intrusion, has produced a strong though disjointed chargeability anomaly halo coincident with an outer pyrite zone that encloses a weaker inner zone (Rice and Sharp, 1976).

A locus taken through all the larger chargeability anomaly centres at Garbh Achadh (A - D in Fig. 9), suggests that they lie on one half of an ellipse of dimensions 0.8 km x 1.1 km that is truncated to the south-east

by the prominent north-east to south-west trending fault. Although of comparatively small areal extent, the size and surface disposition of these anomalies is such that they could be due to the pyritic shell of a small porphyry copper deposit. Similarly, the lower but above background chargeability response over the centre of the intrusion is characteristic of many porphyry coppers.

The hypothesis that chargeability anomalies A to D represent one half of a pyrite shell bisected by faulting would be strengthened if the displaced half could be located. Inspection of the chargeability and resistivity pseudo-section contour patterns related to the prominent fault in the south-east suggests that it dips to the north-west (see for example line 200W). In discussing the results for line 200W (Appendix III) a similar dip is suggested for the co-parallel fault occurring further to the south-east and associated with anomaly E; this fault is not associated with low resistivities. Between these two faults the porphyritic rocks carry insignificant amounts of pyrite, and hydrothermal alteration is limited to widespread development of epidote replacing the mafic constituents. This may indicate downward displacement by post-mineralisation faulting of the epidotic porphyry to its present position adjacent to the pyritiferous, sericitised, biotite-feldspar porphyry north of the prominent fault. However, chargeability values down to the greatest depth investigated are low. This suggests that the truncated half of the biotite-feldspar porphyry (which has been shown to be associated with above background values) does not lie at depth on the down-thrown side of the main fault. It is worth noting that south of the less prominent co-parallel fault, chargeability values are well above background, becoming anomalous in places (F and G in Fig. 9), though these anomalies do not exhibit the same contour pattern in pseudo-section as those clustering about the main biotite-feldspar porphyry. Further

geological mapping and/or shallow drilling over these anomalies should help resolve any association between these anomalies and the intrusion.

DISCUSSION AND CONCLUSIONS

Two distinct types of sulphide mineralisation have been recognised at Garbh Achadh:-

a) a sporadic but persistent strata-bound sulphide mineralisation related to distinct horizons within the Dalradian metasediments and characterised by small pockets of massive replacement pyrrhotite and occasional later veins and impregnations of chalcopyrite.

b) a disseminated sulphide mineralisation associated with the hydrothermal alteration of the biotite-feldspar porphyry intrusion and adjacent aureole rocks and characterised by pyrite with subordinate chalcopyrite and minor molybdenite.

The recognition of sericitic, kaolinitic and very local minor developments of potassic alteration, and their intimate association with the extent and distribution of disseminated sulphides, strongly suggests a 'porphyry copper' style of mineralisation. The generally weak but pervasive sericitic alteration is coincident with widespread but moderate pyrite mineralisation whilst the incidence of chalcopyrite and molybdenite in significant amounts is generally confined to those parts of the intrusion in which kaolinitic alteration and quartz veining are prominent. This is generally on the margins of the intrusion where fracturing and minor faulting are most pronounced. Although there is no positive petrographic evidence, it is believed that downward migration of meteoric water along these fractures has provided a supergene origin for much of the kaolinite.

The lack of a well-defined concentric zonation pattern at Garbh Achadh is probably attributable to the relatively small size of the intrusion ($0.25\ km^2$), the distribution of the igneous breccias, and the regional

metamorphism of the country rocks which has obscured the extent of propylitic alteration within the epidiorites. In addition, the quartzitic composition of the metasediments has rendered them relatively unresponsive to the chemical effects of hydrothermal alteration. Similar characteristics are known to have restricted the development of concentric zoning associated with porphyry style mineralisation at several localities in North America (Guilbert and Lowell, 1974).

The sharp fall in the copper content of the rocks west of the prominent NNE lineament in the north-west sector of the mineralised area, and the lack of significant disseminated sulphides beyond the major ENE fault in the south, also demonstrate that post-mineralisation faulting has imposed important controls on the present limits of the sulphide mineralisation.

The results of the Institute's geophysical investigations proved to be somewhat disappointing. Although the shallow IP anomalies recorded by the earlier company surveys were confirmed, and resistivity surveys were successful in delineating the major faults identified by the photogeological studies, the deeper penetration geophysical investigations did not indicate any appreciable increase in either extent or intensity of sulphide mineralisation. Studies of the chargeability and resistivity pseudo-sections indicate that the geometry of the main conducting sources producing the major anomalies at Garbh Achadh is shallow and 'slab-like'. Consequently it is unlikely that 'porphyry copper' style mineralisation as defined by Lowell and Guilbert (1970) exists there at depth.

In conclusion it can be said that the small areal extent of the surface mineralisation, the low overall grade indicated by the geochemical rock-sampling (nowhere greater than 0.25% Cu), and the lack of a favourable geophysical response at depth provide little encouragement for continued investigations. However, before the economic potential of the area can be

discounted completely the causes of the small geophysical anomalies to the south of the main fault need to be resolved. These occur beyond the limits of the detailed mapping and geochemical grid surveys completed in the current investigation. In addition there is perhaps a case for a modest programme of scout-drilling immediately north of the main fault to test both the prominent IP anomaly there and to investigate the influence on mineralisation of the main fault at depth.

Acknowledgements

The Institute would like to thank the Duke of Argyll for co-operation in permitting the investigations on his estate, and the Forestry Commission for permission to use the access road from Eredine. Access to the confidential reports of Consolidated Gold Fields Limited is gratefully acknowledged.

Thanks are due to U. McL. Michie, P.M. Green, B. Scarth and K. Jacobs who collected the geochemical samples and to the staff of the Analytical and Ceramics Unit who carried out the analytical work.

REFERENCES

COGGAN, J.H. 1973. A comparison of IP Electrode arrays. Geophys. Vol. 38 p. 737-761.

ELLIS, R.A. and others. 1977. Investigation of disseminated copper mineralisation near Kilmelford, Argyllshire, Scotland. Miner. Reconnaissance Prog. Rep. Inst. Geol. Sci. No. 9, 114 pp.

FORTEY, N.J. 1976. Mineralogical investigation of porphyrites and associated rocks from Garbh Achadh, Central Argyllshire. IGS Min. Unit Rep. No. 171 (Unpubl.).

FORTEY, N.J. 1976. Petrographic notes on rock specimens from Garbh Achadh, Argyllshire. IGS Min. Unit Rep. No. 190 (Unpubl.).

GUILBERT, J.M., LOWELL, J.D. 1974. Variations in zoning patterns in porphyry ore deposits. C.I.M. Bulletin pp. 99-109.

HARRIS, A.L., PITCHER, W.S. 1975.. The Dalradian Supergroup. In HARRIS A.L. (Ed.) A correlation of the Pre-Cambrian rock in the British Isles. Geol. Soc. Lond. Spec. Rep. No. 6, p. 52-75.

HAUCK, A.M. 1970. A reconnaissance downhole IP and resistivity survey method. Tech. Paper. McPhar Geophysics Limited, Ontario.

HILL, J.B. and others. 1905. The geology of mid-Argyll. Mem. Geol. Surv. Scotland. No. 37.

JOHNSTONE, G.S. 1966. The Grampian Highlands, 3rd Edtn. Brit. Reg. Geol. 103 pp.

KNILL, J.L. 1963. A sedimentary history of the Dalradian series. In Johnson, M.R.W. and Stewart, F.H. (Eds.). The British Caledonides. Oliver and Boyd, Edinburgh.

LOWELL, J.D., GUILBERT, J.M. 1970. Lateral and vertical alteration - mineralisation zoning in porphyry ore deposits. Econ. Geol. Vol. 65 p. 373-408.

MICHIE, U.McL. and others. 1975. An assessment of the Garbh Achadh project, Argyllshire, Scotland. IGS RMMU Rep. (Unpubl.).

RICE, R., SHARP, G.J. 1976. Copper mineralisation in the forest of Coed-y-Brenin, North Wales. Trans. Inst. Min. Metall. (Sect. B: Appl. Earth Sci.). p. 1-13.

ROBERTS, J.L. 1974. Dalradian structure in the SW Highlands of Scotland. Geol. Soc. Lond. Vol. 130 pt.2. pp. 93-113.

ROBERTS, J.L., TREAGUS, J.E. 1977. Dalradian rocks of the South-West Highlands. Scottish Jnl. Geol. Vol. 13, Pt. 2. pp. 87-99

SMITH, C.G., and others. 1977. Investigation of stratiform sulphide mineralisation in parts of central Perthshire. Miner. Reconnaissance Prog. Rep. Inst. Geol. Sci. No. 8, 83 pp.

TANDY, B.C.,(in preparation). Drainage geochemical survey of central Argyll. Miner. Reconnaissance Prog. Rep. Inst. Geol. Sci.

WILSON, G.V., FLETT, J.S. 1921. The lead, zinc, copper and nickel ores of Scotland. Mem. Geol. Surv. Spec. Rep. Min. Res. G.B. Vol. XVII.

APPENDIX I

1. Locations and descriptions of geochemical samples

POWER AUGERING AND DRILLING - MINUTEMAN RIG June/July 1976

Sample No.	Grid Ref.	Depth (m)	Description
CZS 3190	900 W	0.2	Peat
CZS 3191	00 (O/S 8mE)	0.8	Abundant large clasts of Qtz. schist.
CZD 3073		1.5	Banded phyllitic siltstone with qtz. bands. Lm. strong on fractures.
CZS 3192	800 W	0.9	Peat
CZS 3193	00	1.6	Grey/green clay.
CZD 3074	(O/S 5mN)	2.4/2.7	Foliated epidiorite - no visible sulphides (NVS).
CZD 3075	700 W 00	outcrop	Amphibolite - hackly fractures., Lm. moderate, trace of pyrite.
CZD 3076	600 W 00 (O/S 9mE	outcrop	a) Dk. pinkish grey porphyrite with fresh biotite. Sulphide: sp/tr (Cp?) b) Grey 'peppery' porphyrite with Biotite abundant (2ndry?) NVS.
CZD 3077	500 W 00	outcrop	a) L. brown porphyrite v. fine disseminated py: Sparse. Seric: weak. b) Brown hackly porphyrite Lm: strong. Sc: moderate. Small 2ndry biotites?
CZS 3194	400 W	0.4	Peat with pink felsite fragments.
CZS 3195	00	0.8	Lt. brown sandy clay with some felsite fragments
CZD 3078	(O/S 5mE)	0.8-	Weathered buff felsite (Sc: heavy in phenocrysts) NVS.
CZD 3079		1.2	Cuttings - water-loss heavy.
CZD 3080	300 W 00 (O/S. 5mN)	outcrop	a) Greenish-pink porphyrite (chl. after biotite) Sc: mod. Sulphides: common. b) V. fractured grey porphyrite Lm common in veinlets. Sc: heavy Py: common on fractures.
CZS 3196	200 W	0.9	Peat.
CZS 3197	00	1.7	Grey sandy clay.
CZD 3081		2.3	Greenish pink porphyrite (weathered) chl. thin QV: sp. NVS.
CZD 3082	100 W	1.7/2.2	V. broken banded pelite? NVS.
CZD 3083	100 N	cuttings	O/S 4mW).
CZD 3084	700 W 100 S	outcrop (O/S 10m.S)	Coarse grit NVS
CZS 3198	200 W	1.3	Peat.
CZS 3199	100 N	2.7	Yellowish brown gritty clay (weathered P?).

Sample No.	Grid Ref.	Depth (m)	Description
CZD 3085		3.5	Pale buff porphyrite Sc: heavy, Lm: moderate (staining), pale flecks of dark grey clay material after py. mafics: nil.
CZD 3086	300 W 100 N	0.8/1.2	Highly weathered buff porphyrite Sc: v.heavy Lm: strong Mafics: Nil. NVS.
CZS 3200	250 W	1.4	Peat.
CZS 3201	100 N	2.2	Yellow gritty clay
CZD 3087		2.8	Buff/grey med. grained porphyrite Sc: heavy, Lm: strong. Py: sparse.
CZD 3088	400 W	0.4/0.6	Pinkish brown porphyrite with hackly fractures heavily sericitised feldspar phenocrysts. Lm: moderate/strong. Py: sp.- v. fine dissemination.
CZS 3202	500 W	1.2	Peat
CZS 3203	100 N	1.5	Brown sandy clay with porphyrite fragments. (O/S 8mE). No core.
CZD 3089	O/S 10mN	outcrop	Even-grained dark greenish-grey epidiorite minor 2ndry epidote in small clots. Py: sp/common in lenses and folia.
CZD 3090	700 W	outcrop	Shattered (fractured) pink/grey quartz schist Q.V.: common
	100 N	(O/S 5mE)	Py: sparse/common. (Close to contact).
CZS 3204	800 W	2.5	Peat
CZS 3205	100 N	4.1	Peaty clay
CZD 3091		4.6	Med/coarse-grained Epidiorite. Lm: weak on fractures.
CZS 3206	900 W	0.4	Peat
CZS 3207	100 N	0.7	Grey sandy clay and boulders.
		(O/S 8mS)	
CZD 3092	700 W	outcrop	a) Brownish pink fresh porphyrite. biot/chl: common,Sc: nil.
CZD 3093	200 S		b) Foliated epidiorite. Sulphides: trace.
CZD 3094			c) Buff gritty qtzte. NVS.
CZD 3095	900 W 200 N	(O/S 25mS)	V.coarse pebbly arkosic Qtzte. Sulph: Common/ abundant as strings and large blebs in matrix (Cp. Py. Pyrrh?) occasional pink felspars.
CZD 3096		(O/S 25mE)	Grey fissile grits Py: nil Lm: weak.
CZD 3097		(O/S 30mN)	Dk. greenish-grey foliated epidiorite. NVS.
CZD 3098	800 W	outcrop	Fine, well-bedded arkosic grit Lm: heavy on bedding-planes NVS.
	100 S	(O/S 10mN)	

Sample No.	Grid Ref.	Depth (m)	Description
CZD 3099	600 W	outcrop	a) reddish brown porphyrite Lm: heavy Sc: med/weak Sulph: sparse
	100 S	(O/S 18mS)	b) pinkish brown porphyrite with minor biotite Sc: mod. Sulph: sp.
CZD 3100	400 W	outcrop	Med/cse. brownish pink porphyrite with local
	100 S	(O/S 8mE)	clusters of biotite but mostly chloritised Sc: mod/high in large anhedral felspars. Py: common in large isolated blebs. Incipient miarolitic txt.
CZD 3101	?600 W	outcrop	a) Med/Fine pink porphyrite with incipient
	200 S	(O/S 10mNW)	flow-banding-thin trains of chlorite/epidate. Sulphide: sparse. b) Pink porphyrite/epidiorite breccia, heavily epidotised Sulph: sp/C.
CZS 3208	800 W	4.8	Peat
	200 N		
CZD 3102	700 W	outcrop	Grey hornblende schist with small x cutting qtz veins.
	200 N	(O/S 3mS)	Lm: common on partings. Py: sp/tr.
CZS 3210	600 W	0.1	Peat and brown till.
CZS 3211	200 N	0.8	Brown gritty sand with clasts of biotitic porphyrite.
CZD 3103		cuttings	
CZD 3104		1.3/2.4	Grey porphyrite - with white powdery Feldspar phenocrysts Sc: v.hvy Mo: in thin veinlets.
CZD 3105	600 W	600 W	Pink biotite porphyrite Sc: moderate/heavy
	220 N		Qv. occasional. Sulphide: blebs of Cp. common. Mct.- common as stains on felspars.
CZS 3212	500 W	1.7	Peat
CZS 3213	200 N	2.1	Brown silty clay.
CZD 3106		2.8	Brecciated pale green epidiorite in siliceous matrix Py: v. common.
CZD 3107	400 W	outcrop	Fe-stained biotite porphyrite criss-crossed with thin hair fractures. Sc: weak. Sulphides:
	200 N	(O/S 18m70°)	Cp. common. Mct: common.
CZD 3108	00	outcrop	Amphibolite (2ndry? epidote).
	200 N		
CZD 3109	00	outcrop	Grey qtzte with Q.V. and Py veinlets common.
	300 N		Lm: common.
CZD 3110	00	outcrop	Pinkish brown Porphyrite with Ho and chl. and occasional biot.
	400 N	(O/S 20mN)	Sc: moderate Py: sp. as distinct blebs in groundmass.
CZD 3111	100 W	outcrop	Sheared silicified grit Lm: strong on frac-
	200 N		tures. NVS.

Sample No.	Grid Ref.	Depth (m)	Description
CZS 3214	300 W	0.5	Peat
CZS 3215	200 N		Brown silty clay with porphyrite fragments.
CZS 3216	250 W	1.8	Peat
CZS 3217	200 N	3.0	Peat and felsite fragments
CZD 3112		3.35	Grey/pink biotite porphyrite with minor Q.V. Sc. mod Py. Sp.
CZS 3218	200 W	1.9	Peat
CZS 3219	200 N	2.3	Grey Clay
CZD 3113	(O/S 60mSE)	outcrop	Epidiorite sulphide: sp but common fractures.
CZD 3114	100 W 400 N	outcrop (O/S 10mN)	Foliated epidiorite Py: tr.
CZD 3115	00 500 N	outcrop (O/S 15mE)	Epidiorite with Q.V. and inclusion of qtzte. Lm. hvy. NVS.
CZD 3116	100 W 300 N	Scree	Epidiorite Py: sp/tr.
CZD 3117	250 W 300 N	outcrop	Partially foliated epidiorite Py: sp/tr.
CZS 3220	200 W	2.1	Peat
CZS 3221	300 N	4.0	Brown gritty clay with pyritous porphyrite fragments.
CZS 3222	300 W	1.6	Peat
CZS 3223	300 N	2.0	Green peaty clay.
CZD 3118	350 W 250 N	outcrop	Greyish pink fractured porphyrite with biotite minor Q.V. with mo. Cp. common. Mct. v. common.
CZS 3224	350 W	0.8	Peat
CZS 3225	300 N	1.5	Weathered porphyrite.
CZS 3226	400 W	0.4	Peat
CZS 3227	300 N	1.0	Yellow sandy clay with porphyrite fragments.
CZS 3228	500 W	0.9	Yellow sand
CZS 3229	300 N	2.0	Grey clay
CZS 3230	600 W	1.5	Peat
CZS 3231	300 N	2.2	Peaty clay
CZD 3119	900 W 400 N	outcrop (O/S 20mNE)	a) Grit with lge Q.V. NVS. b) Grey/green tuff? NVS.
CZD 3120	800 W 500 N	outcrop	Cse. well-bedded sst Lm: moderate NVS
CZD 3121	700 W 500 N	outcrop	Grit NVS

Sample No.	Grid Ref.	Depth (m)	Description
CZD 3122	600 W 400 N	outcrop (O/S 11mSE)	Foliated siltstone. Py: tr.
CZD 3123	(O/S 20mSE)	outcrop	Indurated, fractured epidiorite Lm: heavy. Sulphides: Ab.
CZD 3124	475 W 385 N	outcrop	Pinkish brown porphyrite heavily chloritised Sc: mod. Py: Sp. Lm. weak.
CZD 3125	400 W 500 N	outcrop (O/S 12mSW)	Rubbly, weathered buff porphyrite Sc: v.heavy Lm: strong. Py: common.
CZD 3126	400 W 400 N	outcrop (O/S 6mN)	Dark pinkish brown biotic porphyrite. Py: tr. Sc: weak.
CZD 3127	200 E 500 N	outcrop	'Rusty' epidiorite Py; sp
CZD 3128	100 E 400 N	outcrop	Cse fractured grit Lm: v.strong. NVS (fault-zone?)
CZD 3129	120 E 290 N	outcrop	Hackly epidiorite with epidote. Py: common on fractures.
CZD 3130	500 W 100 S	outcrop	Hackly epidiorite Lm: moderate Py: sp.
CZS 3232	100 W 500 N	1.8	Peat
CZS 3234	200 W	1.0	Peat
CZS 3235	500 N	1.6	Grey gritty clay
CZS 3236	300 W	0.3	Peaty/clay
CZS 3237	500 N	0.8	Orange clay
CZD 3131	200 W 400 N	outcrop	Hornblende schist NVS.
CZS 3238	300 W	0.5	Peat
CZS 3239	400 N	1.4	Brown clay with clasts of qtzte and epidiorite
CZD 3132	500 W 500 N	(O/S 25mE)	Pink porphyrite Py: sp
CZS 3240	700 W	0.6	Peat
CZS 3241	300 N	1.0	Grey/green till
CZD 3133	800 W 283 N		Sst NVS.
CZS 3242	283 N	0.4	Yellow silty clay.

Sample No.	Grid Ref.	Depth (m)	Description
CZD 3134	600 W 300 S	outcrop (O/S 10mNE)	Pink brown porphyrite breccia with epidote Py; sp
CZS 3244	700 W	1.3	Peat
CZS 3245	400 N	1.9	Grey clay with epidiorite clasts.
CZS 3246	800 W	0.6	Peat (adjacent drainage ditch)
CZS 3247	400 N	1.0	Brown clay with qtzte fragments.
CZS 3248	900 W	2.8	Peat
CZS 3249	300 N	3.6	Green clay (weathered epidiorite?)
CZD 3135	800 W 500 S	outcrop	Amphibolite? NVS
CZD 3136	800 W 320 S	outcrop	Pink biotite porphyrite Py: common
CZD 3070	600 W 100 N	outcrop	Dk. grey biotite porphyrite Sc: weak Py: sp/c (Cp?) in veinlets and dissems
CZD 3071	600 W 900 N	outcrop	Banded quartz schist
CZD 3072	600 W 500 N		Grit NVS
CZR 806	645 W 385 S	outcrop	Porphyry
CZR 808	450 W 175	outcrop	Epidotised banded quartzite
CZR 809	620 W 020 N	outcrop	Igneous breccia
CZR 812	610 W 010 N	outcrop	Porphyry
CZR 849	500 W 320 N	outcrop	Epidiorite

2. Analytical results of geochemical samples

Stream sediment samples

	Cu	Zn	Ni
CZC1208	60	400	75
CZC1223	25	340	60
CZC1229	5	80	40
CZC1231	75	400	75
CZC1232	10	110	45
CZC1238	200	300	50
CZC1240	320	190	60
CZC1242	45	130	55
CZC1245	145	210	50
CZC1247	100	180	50
CZC1251	40	100	55
CZC1254	70	200	60
CZC1255	55	180	55
CZC1258	25	140	45
CZC1261	80	150	100
CZC1266	60	200	65
CZC1268	105	160	55
CZC1271	105	170	50
CZC1277	65	300	75
CZC1280	60	170	75
CZC1285	20	270	45
CZC1288	40	200	60

Peat and till samples

	Cu	Pb	Zn	Ag
CZS3190	45	40	20	0
CZS3191	200	20	20	2
CZS3192	320	20	30	1
CZS3193	730	10	50	2
CZS3194	35	20	40	2
CZS3195	170	20	60	10
CZS3196	260	20	30	1
CZS3197	330	20	50	2
CZS3198	65	30	30	1
CZS3199	50	20	20	5
CZS3200	50	20	30	1
CZS3200	50	20	30	1
CZS3201	250	40	60	3
CZS3202	210	20	50	2
CZS3203	470	20	60	6
CZS3204	100	10	10	1
CZS3205	1560	10	50	2
CZS3206	90	50	20	0
CZS3207	230	20	30	2
CZS3208	445	10	80	1
CZS3210	100	20	20	1
CZS3211	515	10	20	2
CZS3212	1285	20	30	1
CZS3213	2020	20	40	2
CZS3214	45	20	10	0
CZS3215	310	30	60	1
CZS3216	20	10	10	0

	Cu	Pb	Zn	Ag
CZS3217	195	20	20	1
CZS3218	225	30	40	1
CZS3219	470	10	90	1
CZS3220	75	20	20	1
CZS3221	205	20	80	1
CZS3222	20	10	10	0
CZS3223	625	10	80	1
CZS3224	50	10	10	0
CZS3225	210	10	30	1
CZS3226	900	30	50	1
CZS3227	335	10	30	2
CZS3228	1005	10	20	1
CZS3229	1075	10	10	1
CZS3230	295	10	10	2
CZS3231	1260	40	40	2
CZS3232	105	10	20	1
CZS3234	420	50	20	1
CZS3235	755	20	50	1
CZS3236	130	20	60	1
CZS3237	645	20	30	1
CZS3238	50	20	10	0
CZS3239	620	30	80	1
CZS3240	30	10	10	0
CZS3241	170	20	40	1
CZS3242	50	20	30	0
CZS3244	10	20	10	1
CZS3245	55	30	70	1
CZS3246	5	20	10	0
CZS3247	5	20	20	1
CZS3248	15	10	40	1
CZS3249	25	20	70	1

Rock samples

	Cu	Pb	Zn	Ag	Co	Ni	Mo
CZD3070	340	10	10	1	15	10	9
CZD3071	30	10	20	0	5	10	5
CZD3072	5	10	10	0	0	5	3
CZD3073	105	10	10	1	10	40	10
CZD3074	100	10	30	1	25	85	4
CZD3075	80	10	40	1	30	85	10
CZD3076	25	20	20	1	5	10	5
CZD3077	10	10	20	1	6	15	4
CZD3078	45	10	10	1	10	20	3
CZD3079	100	20	40	6	10	25	4
CZD3080	25	10	30	0	10	15	2
CZD3081	10	20	20	0	10	15	3
CZD3082	680	10	30	1	30	70	21
CZD3083	1075	20	40	5	55	90	33
CZD3084	5	10	5	0	5	0	1
CZD3085	15	10	10	1	10	10	4
CZD3086	275	30	40	0	5	10	9
CZD3087	100	30	20	0	10	10	1
CZD3088	15	10	20	0	10	10	0
CZD3089	60	10	20	1	25	70	3

	Cu	Pb	Zn	Ag	Co	Ni	Mo
CZD3090	135	10	10	0	5	15	9
CZD3091	150	10	20	1	20	40	3
CZD3092	5	10	30	0	10	10	7
CZD3093	150	20	20	1	45	60	9
CZD3094	10	10	0	0	5	5	6
CZD3095	185	10	10	0	5	5	2
CZD3096	10	10	10	0	5	5	4
CZD3097	5	20	30	0	15	5	5
CZD3098	45	10	0	0	5	5	37
CZD3099	5	20	20	0	5	15	2
CZD3100	70	20	30	0	5	10	2
CZD3101	30	10	30	0	10	30	4
CZD3102	125	10	10	0	15	35	6
CZD3103	1920	10	240	1	85	60	38
CZD3104	1130	10	10	1	10	15	574
CZD3105	2450	10	20	2	10	15	8
CZD3106	240	20	20	1	15	60	12
CZD3107	120	20	30	0	25	40	7
CZD3108	1190	20	20	1	10	15	5
CZD3109	95	10	20	0	15	50	2
CZD3110	10	10	30	0	5	15	6
CZD3111	75	10	0	0	0	5	10
CZD3112	10	10	10	0	0	0	4
CZD3113	315	10	20	0	5	15	8
CZD3114	90	10	20	1	30	140	4
CZD3115	55	10	40	1	30	20	2
CZD3116	55	10	20	1	20	75	2
CZD3117	80	20	20	1	30	90	7
CZD3118	2000	10	20	2	5	10	41
CZD3119	15	10	30	0	5	5	3
CZD3120	10	10	10	0	5	5	1
CZD3121	10	10	10	0	5	10	3
CZD3122	25	10	20	0	10	30	6
CZD3123	400	20	20	1	25	10	17
CZD3124	15	10	30	0	5	10	1
CZD3125	5	20	10	0	5	10	5
CZD3216	20	10	30	1	10	10	2
CZD3127	25	20	40	1	30	90	4
CZD3128	10	20	5	0	0	5	4
CZD3129	10	20	30	1	20	60	3
CZD3130	60	20	30	1	30	130	4
CZD3131	50	10	30	0	10	30	4
CZD3132	5	10	30	1	5	10	5
CZD3133	15	10	30	1	10	30	4
CZD3134	340	10	20	1	10	15	13
CZD3135	50	10	30	0	25	50	3
CZD3136	15	20	20	0	5	10	4
CZR 806	570						35
CZR 808	2130						600
CZR 809	810						95
CZR 812	1590						195
CZR 849	1600						

APPENDIX II

Mineralogical descriptions of rock specimens

Sample locations for the specimens described below in Table 1 are given in Fig. 5. The majority of the rocks are variously altered porphyries of dacitic character. It is probable that tonalitic and rhyodacitic types are present, but the present data are insufficient to resolve this question.

In the table the following symbols and abbreviations are employed:-

1. Alteration - Plag. (plagioclase) : A - mildly sericitised; B - strongly sericitised; C - minor kaolinitisation; D - advanced kaolinitisation.

2. Alteration - Mafic : A - primary mafic phenocrysts are preserved; B - chloritic pseudomorphs; C - sericite/muscovite pseudomorphs; D - advanced alteration of uncertain status.

3. Alteration - Epid. (Epidote) : A - minor amount of epidote present; B - epidote is a major constituent; n.d. - not located.

   Combined symbols are used to denote complex types of alteration.

4. Ore/opaque minerals : P - pyrite; cp - chalcopyrite; cov - covellite; po - pyrrhotite; sp - sphalerite; ars - arsenopyrite; moly- molybdenite; ilm - ilmenite; mag - magnetite; hm - hematite; goet - goethite; nd - barren.

5. Assay data : min - minor amount (not more than 200 ppm Cu); tr - minute amount (less than 50 ppm Cu); figures refer to amounts in ppm; nd - not detected.

APPENDIX II : Table 1: Summary of Mineralogical Data on Selected Rock Specimens.

Specimen No.(CZR)	Rock Type	Alteration			Ore/Opaque Minerals	Assays (qual. & ppm)		
		Plag.	Mafic	Epid.		Cu.	Ni.	Mo.
805	Hornblende-diabase with epidote ('epidiorite').	-	-	A	Ilm, mag, py, cp	min	nd	nd
806	Intensely altered porphyry with syn-alteration disruption.	A/B	D	n.d.	Py, cp (moly)	570	nd	35
807	Flow banded, altered porphyry.	A	B	n.d.	Py, cp	min	nd	nd
808	Epidotised banded quartzite .	-	-	B	Py, cp, moly, cov, sp.	2130	nd	600
809	Volcanic breccia with fragments of porphyry and host sediment.	A	A	A	Py, cp.	810	nd	95
810	Altered porphyry with biotite of likely secondary origin.	C	D	n.d.	Py, cp	min	nd	tr
811	Epidote-rich volcanic breccia with porphyry and sediment fragments.	B	B	B	Py	-	-	-
812	Altered porphyry with primary biotite.	D	D	n.d.	Py, cp, moly, cov mag.	1590	n.d.	195
831	Quartzite & schist with sulphide bearing quartz veins.	-	-	-	Py, cp, po, ars, sp.	21500 132000	20500 7400	n.d. n.d.

Specimen No.(CZR)	Rock-type	Alteration			Ore/Opaque Minerals	Assays (qual & ppm).		
		Plag.	Mafic	Epid.		Cu	Ni	Mo
837	Altered dacitic porphyry	B	B	n.d.	Py	min	nd	nd
838	Quartzite	-	-	n.d.	Py	min	nd	nd
839	Altered dacitic porphyry	D	B/C	n.d.	Py	tr	nd	nd
840	Altered dacitic porphyry crossed by hair veinlets of goethitic clay	D	B	n.d.	Py, cp.	min	nd	nd
841	Altered dacitic porphyry	C	B	B	n.d.	-	-	-
842	Cu-bearing limonitic gossan with fragments of quartzite	-	-	-	goet	1820	nd	nd
843	Quartzite with banded development of sulphide	-	-	-	Py, cp, po	6990	n.d.	nd
844	Altered dacitic porphyry	A	B	A	Py	-	-	-
845	Biotite-porphyry with a ground-mass of microgranophyre	B/C	A	B	Py	nd	nd	nd
846	Altered dacitic porphyry rich in xenolithic fragments of quartzite	A	B	B	Py	-	-	-
847	Biotite bearing dacitic porphyry	A	B	n.d.	Py	tr	nd	nd
848	Altered dacitic porphyry	A/C	C	n.d.	Py	tr	nd	nd

Specimen No.(CZR)	Rock-type	Alteration			Ore/Opaque Minerals	Assays (qual. & ppm).		
		Plag.	Mafic.	Epid.		Cu	Ni	Mo
849	Flow-banded epidote-bearing diabase (epidiorite).	-	-	A	Py, cp, po	1600	nd	nd
857	Biotite-bearing dacitic porphyry.	A/C	B	n.d.	Py	-	-	-
858	Inter-banded actinolite and sericite; epidote and ferrian-zoisite present.	-	-	B	Py	-	-	-
863	Porphyry in which alteration changes in response to quartz veins.	B/C	C/A	n.d.	Py, malachite	-	-	-
864	Biotite-bearing dacitic porphyry.	A	A/B	n.d.	Py, cp, malachite	-	-	-
867	Biotite-bearing dacitic porphyry.	A/C	A	n.d.	Py,cp,malachite	-	-	-
868	Biotite-bearing dacitic porphyry.	D	A	n.d.	Py	-	-	-
870	Epidote-rich chloritic rock with traces of banding.	-	-	13	Py, cp, hm	-	-	-
871	Altered dacitic porphyry	D	C	n.d.	Py, cp	-	-	-
879	Brecciated sediment with epidote, zoisite, actinolite, albite, etc.	-	-	B	Hm, py, cp	-	-	-
881	Banded metasediment in which banded sulphide is common	-	-	n.d.	Py, cp, hm	-	-	-
882	Epidote-rich random textured rock; possibly a volcanic breccia.	-	-	B	Py. cp.	-	-	-

APPENDIX III

GEOPHYSICAL SURVEY RESULTS

Figs. A3.1 - A3.11 present total intensity magnetic field profiles and apparent resistivity and chargeability pseudo-sections for each traverse. A detailed discussion of the pseudo-sections is given in the text which follows the figures.

The legend below refers to Figs. A3.1 - A3.11

Magnetic Field Profiles: All total intensity magnetic field values have been corrected for diurnal variation and reduced to a single base. Units of field are nanotesla (nT) where 1nT = 1 gamma.

Resistivity and I.P. Sections: Pseudo-sections of apparent resistivity in ohm metres and chargeability (M_{240}^{1140}) in milliseconds are presented.

Horizontal scale: 1:5000

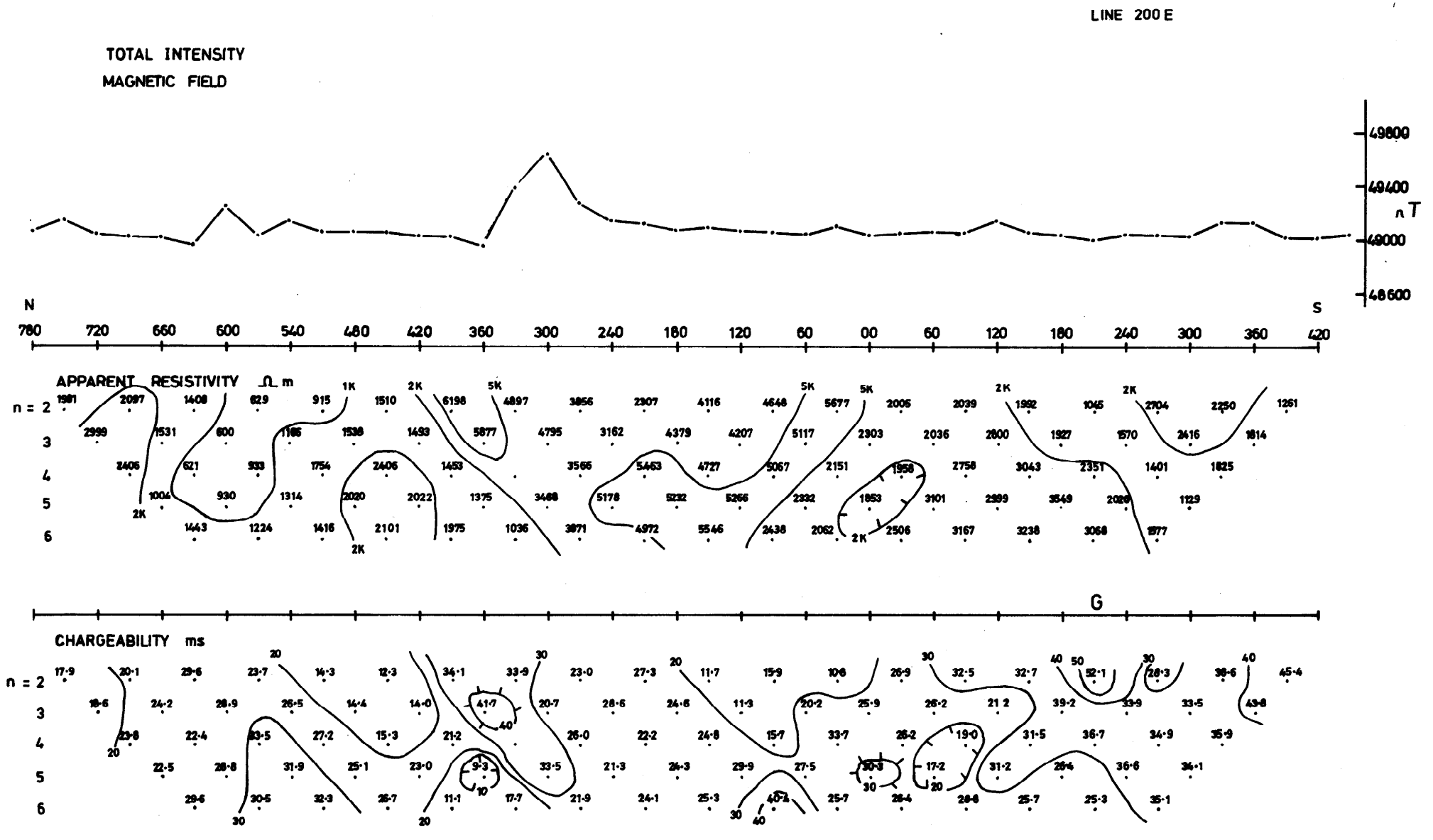

Fig. A3·1 TOTAL INTENSITY MAGNETIC FIELD PROFILE AND APPARENT RESISTIVITY, CHARGEABILITY PSEUDO SECTIONS LINE 200E

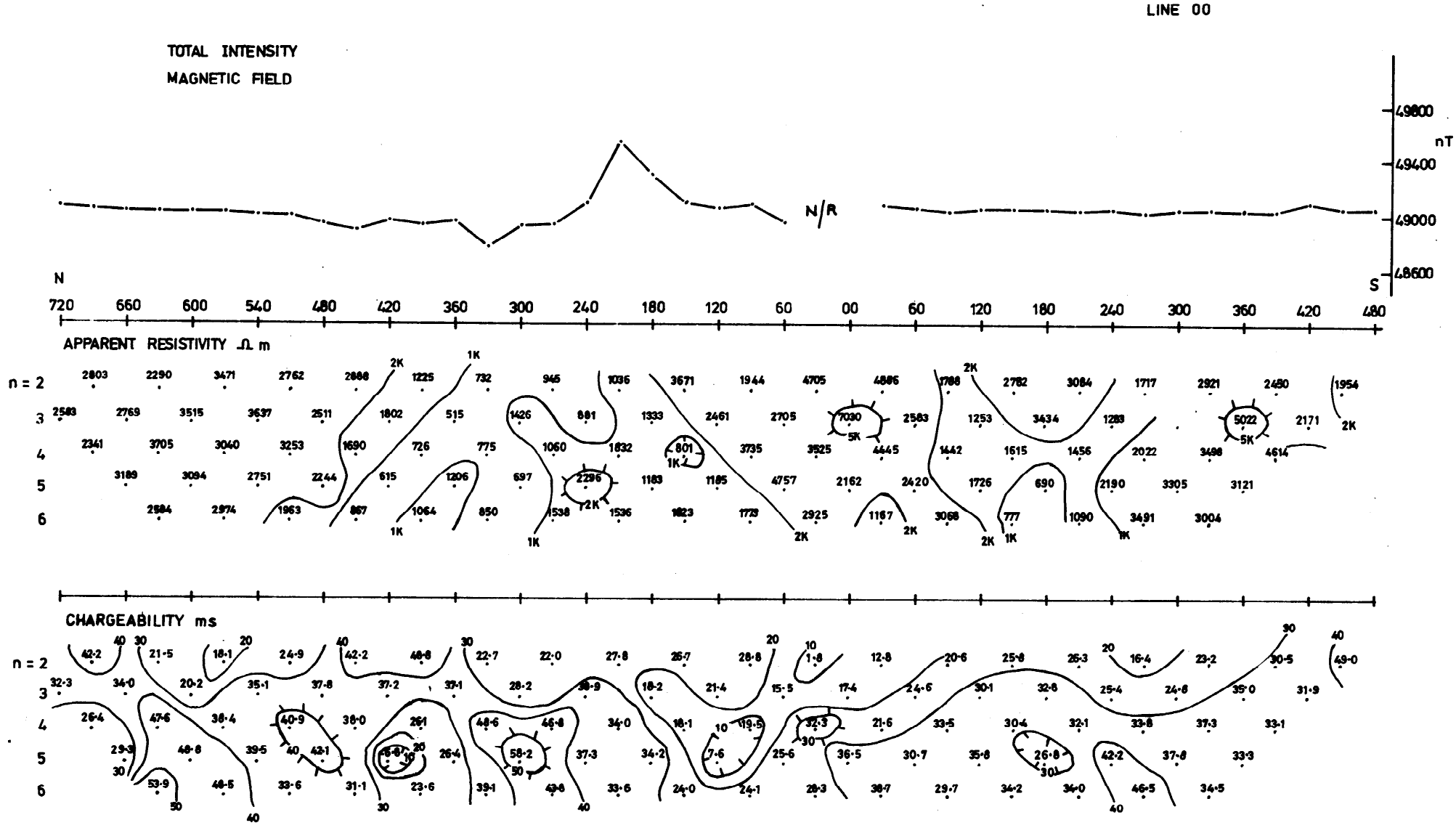

Fig. A3·2 TOTAL INTENSITY MAGNETIC FIELD PROFILE AND APPARENT RESISTIVITY, CHARGEABILITY PSEUDO SECTIONS FOR LINE 00

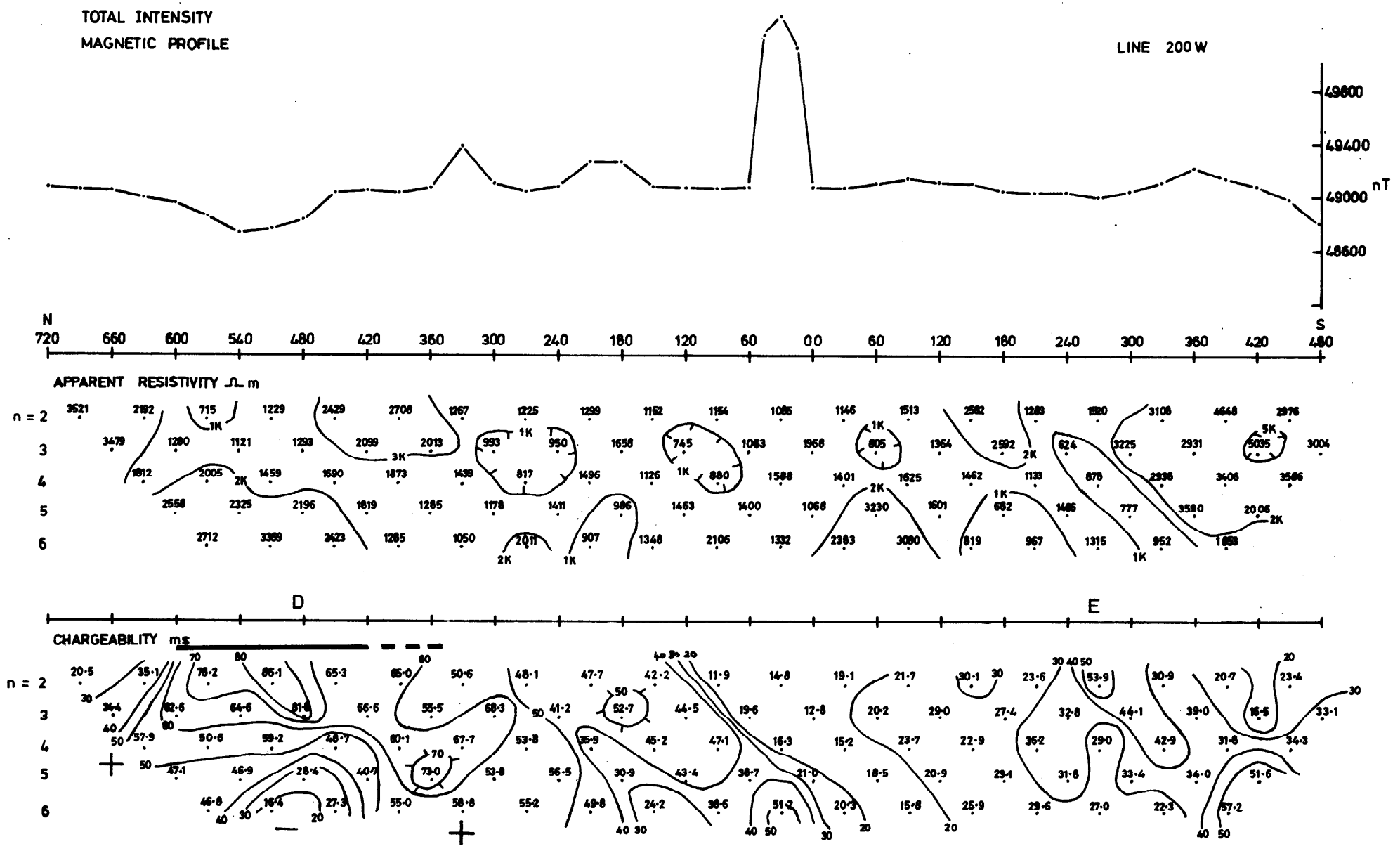

Fig. A3·3 TOTAL INTENSITY MAGNETIC FIELD PROFILE APPARENT RESISTIVITY AND CHARGEABILITY PSEUDO SECTIONS FOR LINE 200W

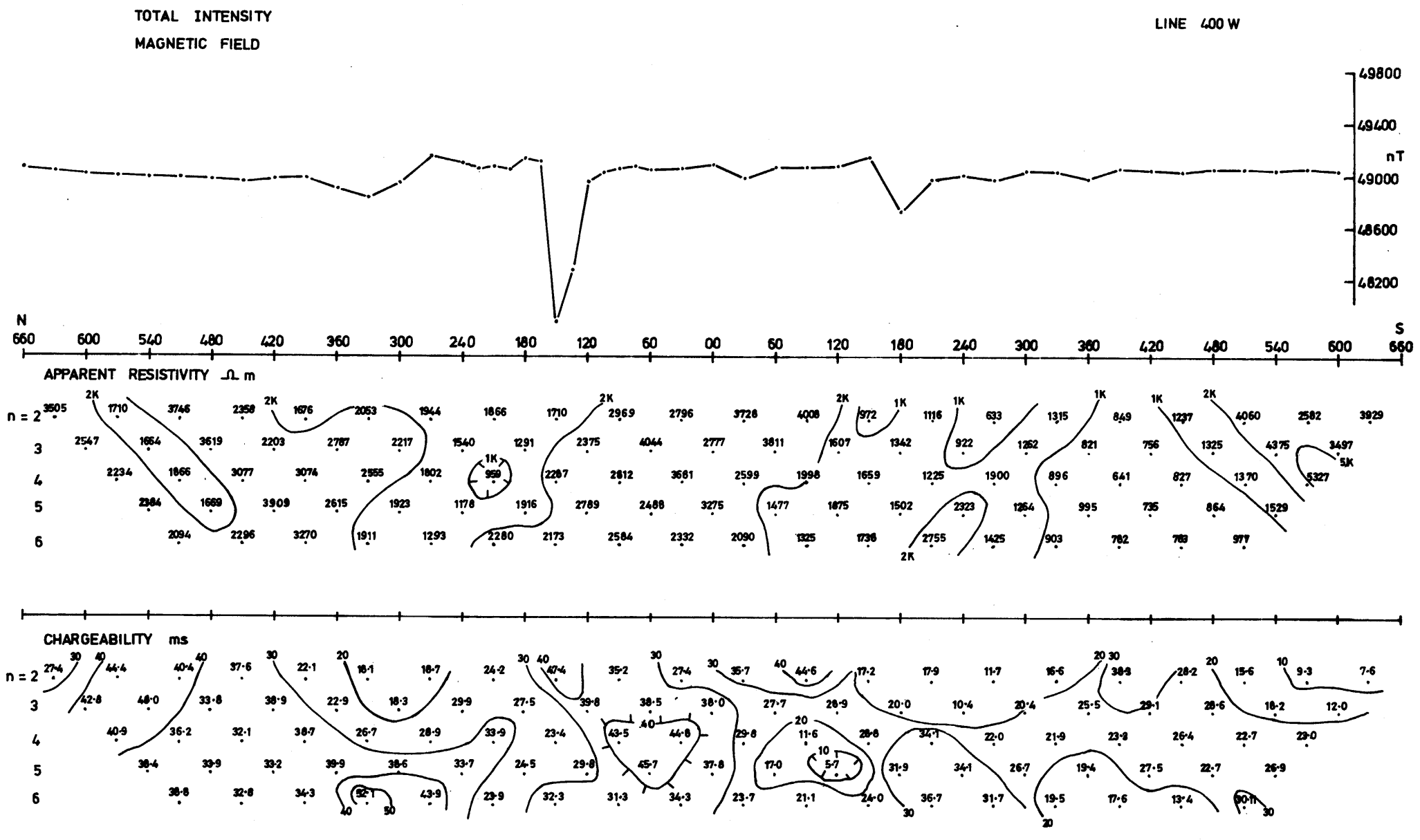

Fig. A3·4 TOTAL INTENSITY MAGNETIC FIELD PROFILE AND APPARENT RESISTIVITY CHARGEABILITY PSEUDO SECTIONS FOR LINE 400W

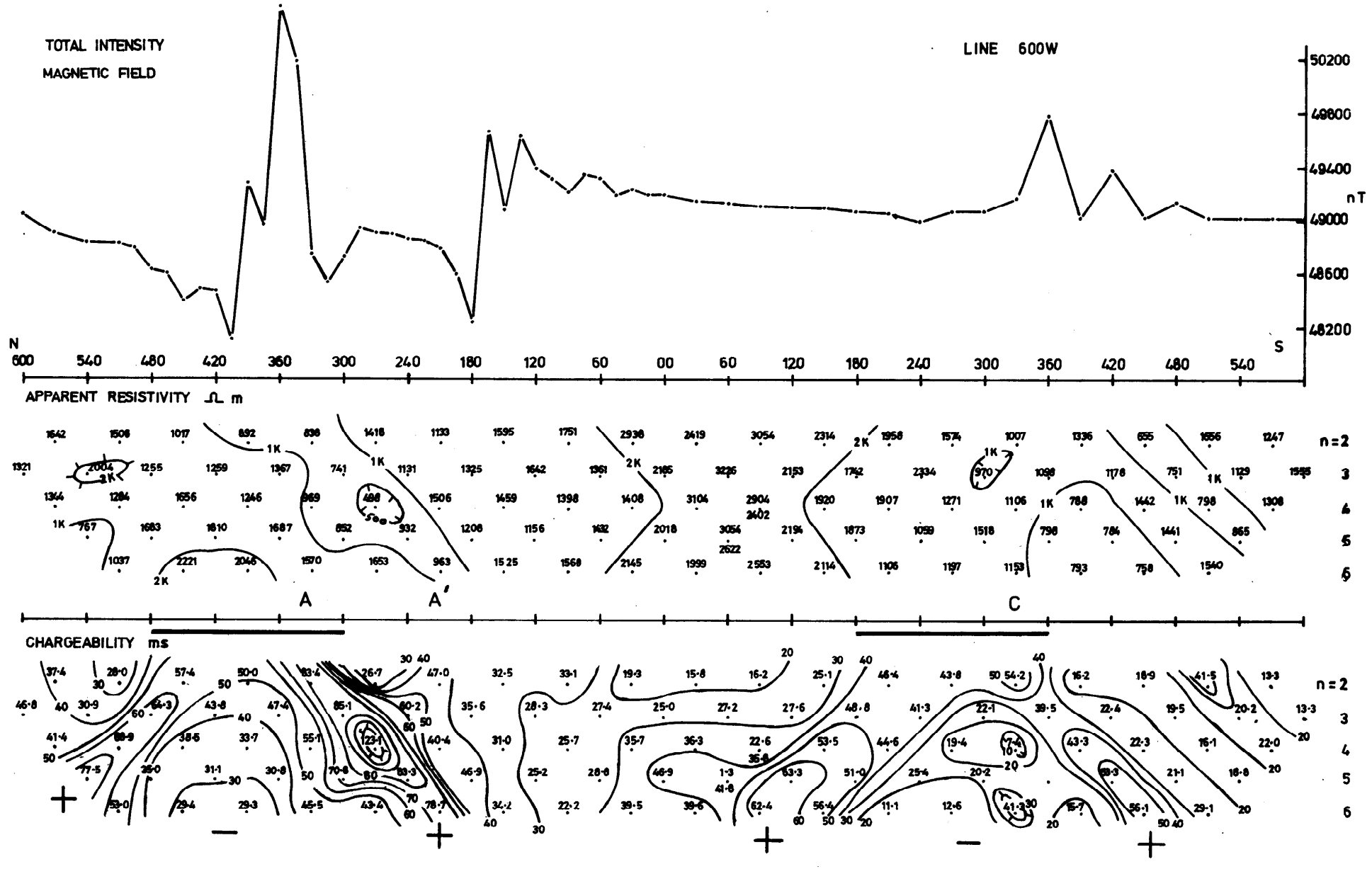

Fig. A3·5 TOTAL INTENSITY MAGNETIC FIELD PROFILE AND APPARENT RESISTIVITY, CHARGEABILITY PSEUDO SECTIONS FOR LINE 600W

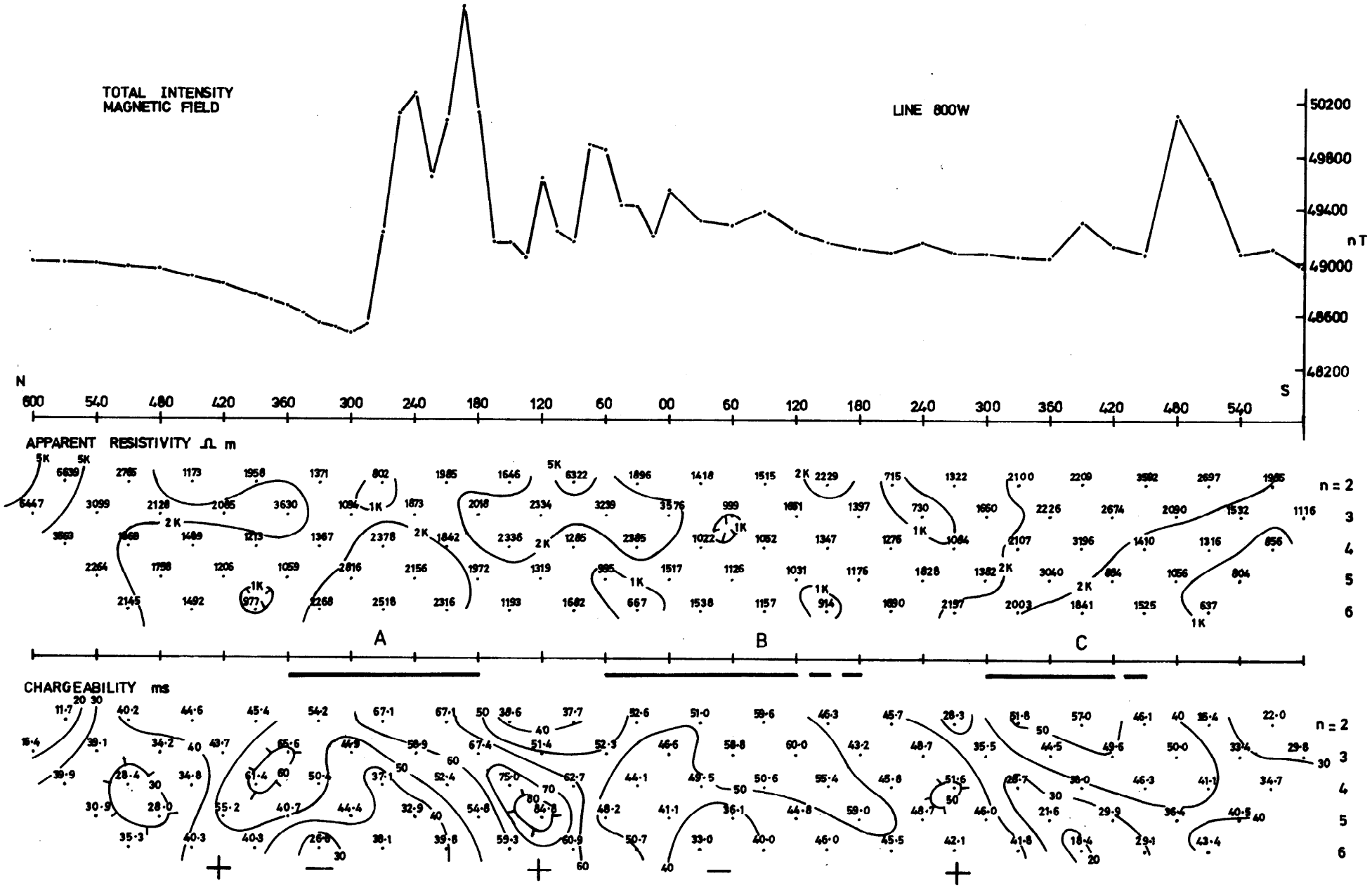

Fig. A3·6 TOTAL INTENSITY MAGNETIC FIELD PROFILE AND APPARENT RESISTIVITY, CHARGEABILITY, PSEUDO SECTIONS FOR LINE 800W

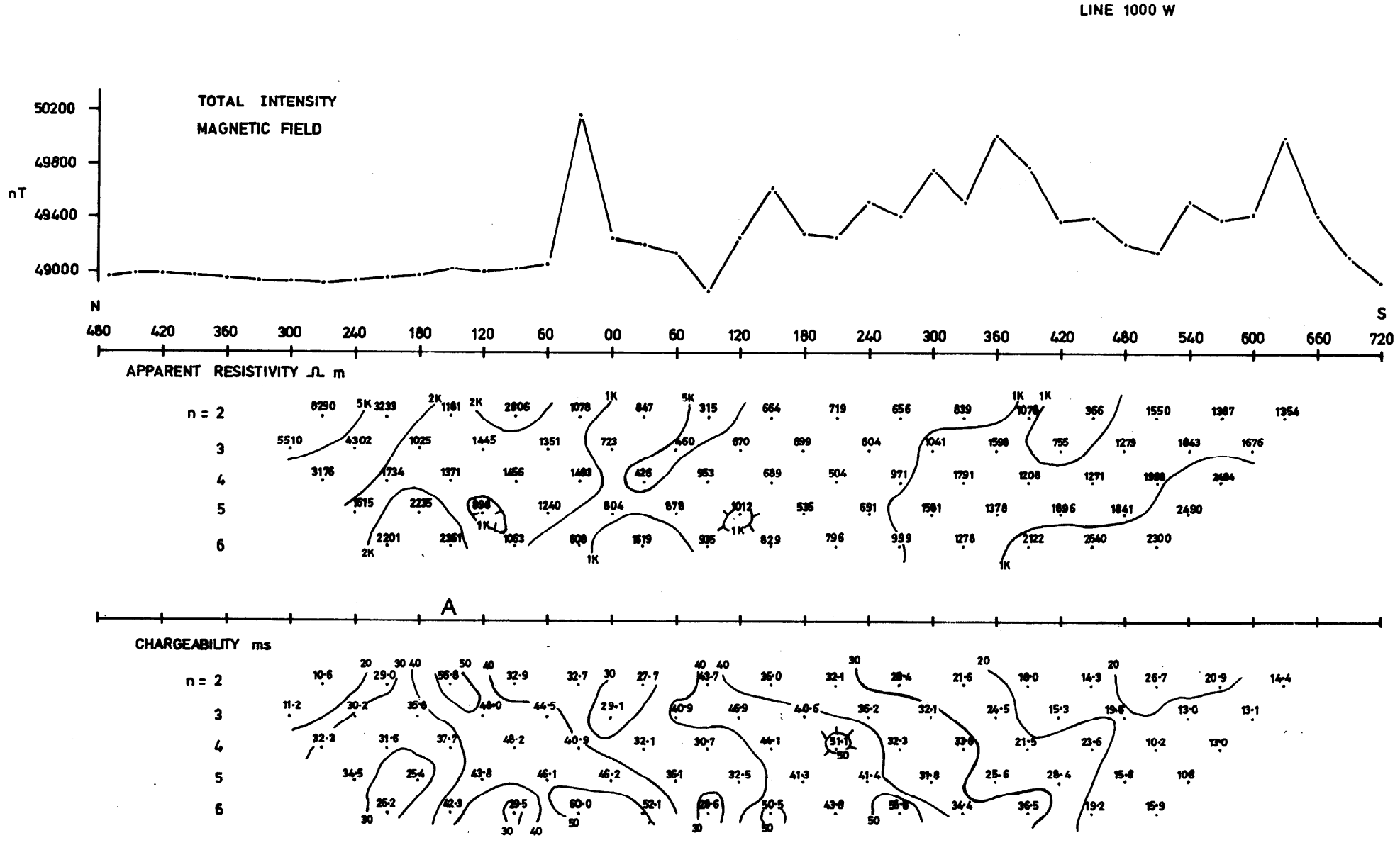

Fig.A3·7 TOTAL INTENSITY MAGNETIC FIELD PROFILE AND APPARENT RESISTIVITY, CHARGEABILITY PSEUDO SECTIONS LINE 1000W

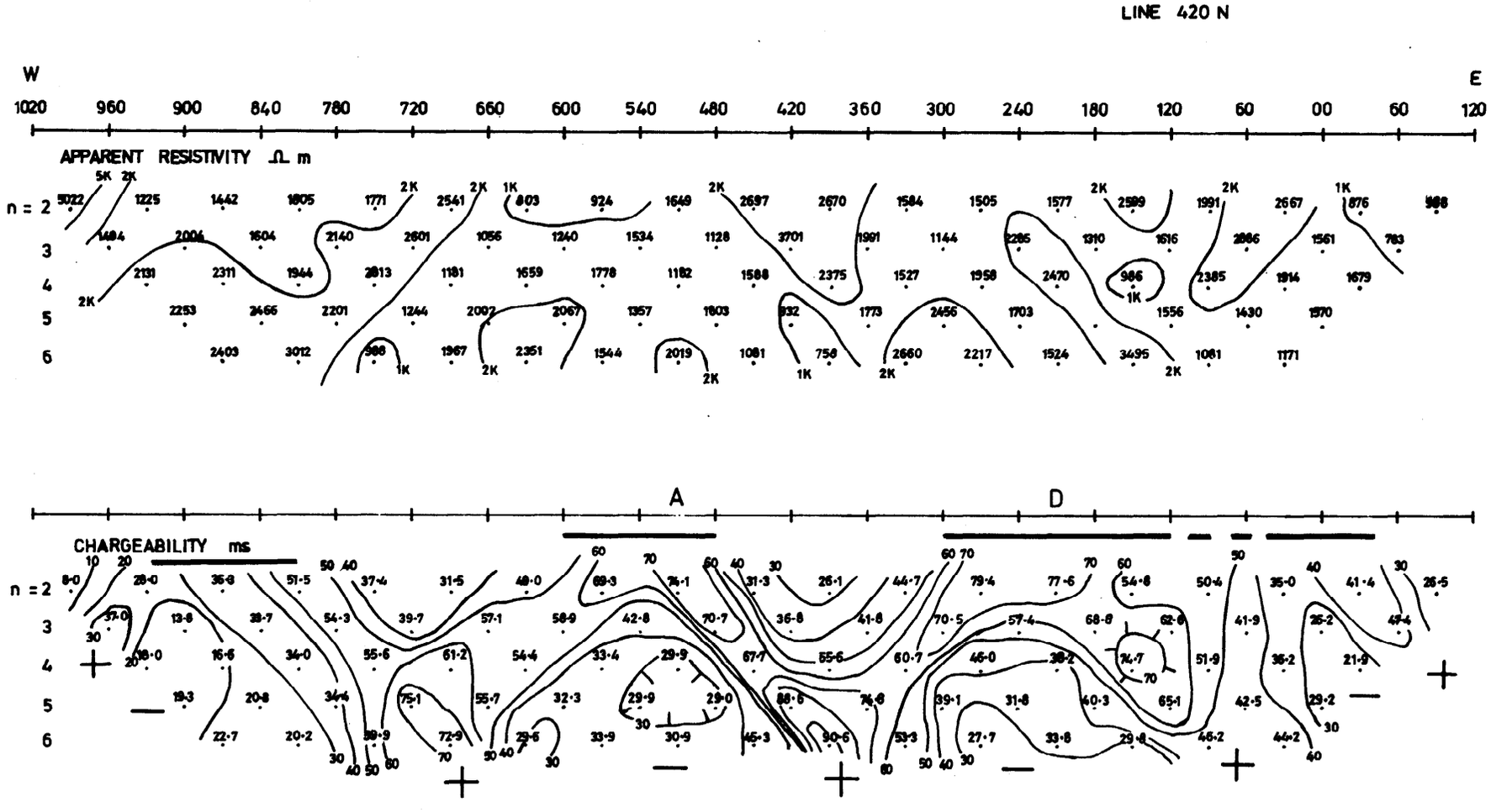

Fig.A3·8 APPARENT RESISTIVITY AND CHARGEABILITY PSEUDO SECTIONS FOR LINE 42ON

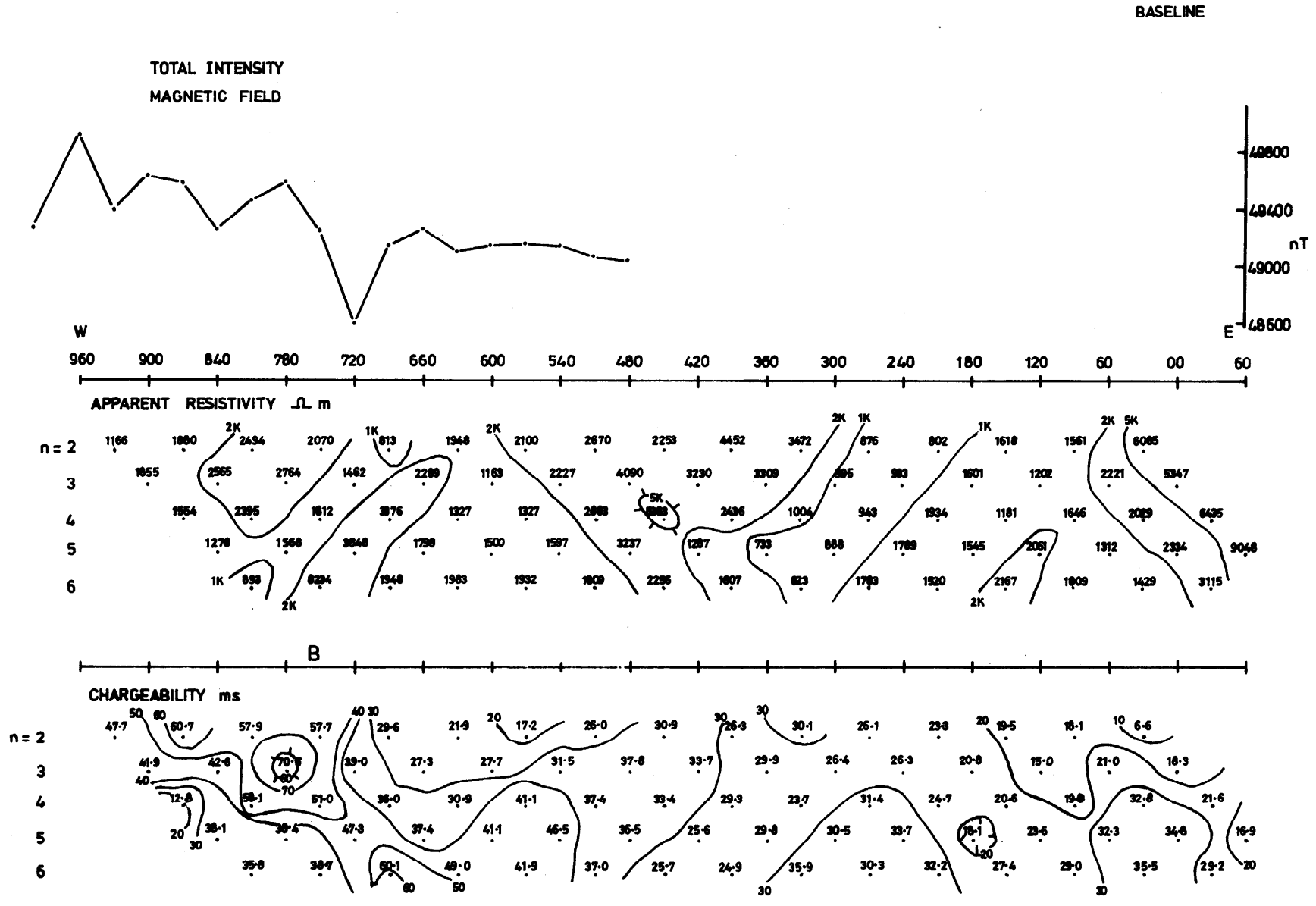

Fig. A3·9 TOTAL INTENSITY MAGNETIC FIELD PROFILE AND APPARENT RESISTIVITY, CHARGEABILITY PSEUDO SECTIONS FOR BASELINE

LINE 420 S

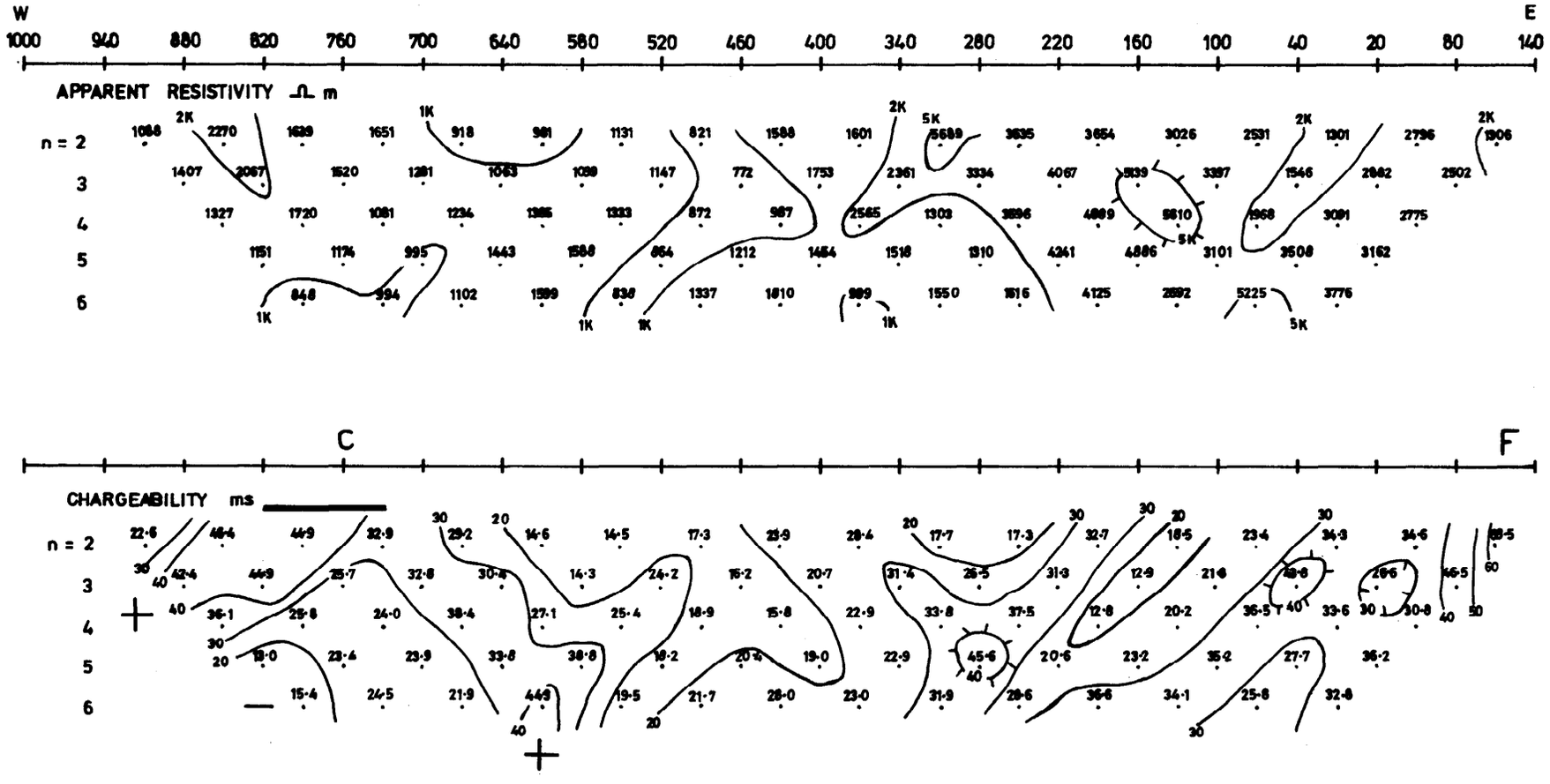

Fig. A3·10 APPARENT RESISTIVITY AND CHARGEABILITY PSEUDO SECTIONS FOR LINE 420S

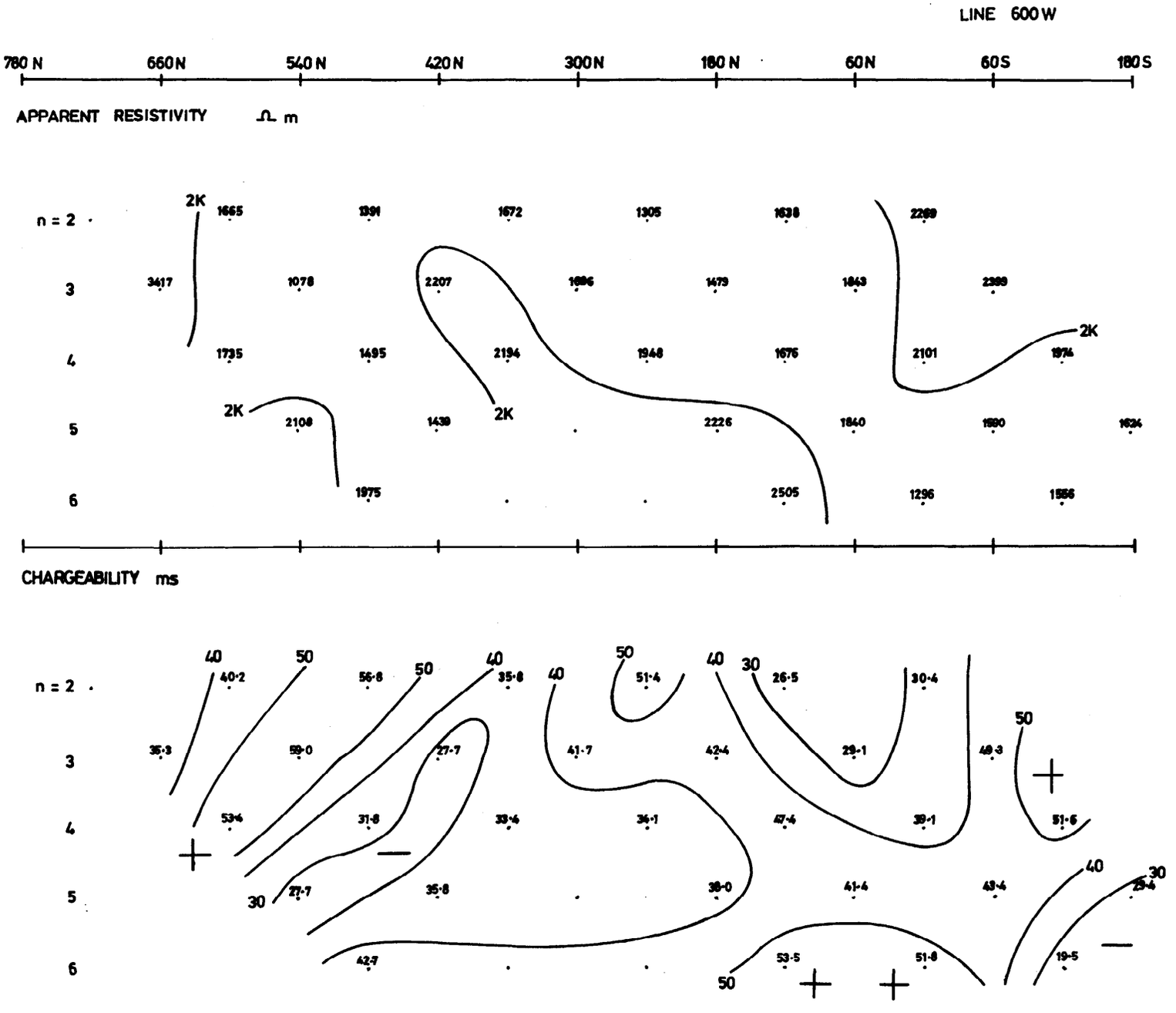

Fig. A3·11 LARGE DIPOLE (120m) APPARENT RESISTIVITY AND CHARGEABILITY SECTIONS FOR PART OF LINE 600W

Discussion of pseudo-sections

Chargeability anomalies on pseudo-sections which correspond with those shown on the contour plan for n=2, (Fig. 9), have been labelled with the same letters. These anomaly contour patterns on the pseudo-sections have then been compared with patterns from 'known geometry' IP models. It is emphasised here that the position and value of each data point should not be thought of as representing that point alone, but rather the integrated effects of the whole volume of earth between the dipole electrodes as well as to each side of the line joining the dipoles. Also, the interpreted near-surface lateral extent of an anomalous zone (denoted by a thick horizontal line on the pseudo-sections) may only be established to an accuracy of one dipole length increasing to over two dipole lengths for buried, dipping and/or gradational contacts.

A discussion of the salient features and suggested sources is now given for each traverse.

Line 200E

This profile has a mean chargeability value of a little over background (Fig. A3.1). The resistivity low, extending to depth between 600N and 480N, corresponds to the main north-east to south-west trending fault (hereafter called the main fault). At 360N shallow sub-anomalous chargeabilities that extend to depth coincide with a magnetic anomaly centred over probable epidiorite. The shallow chargeability lows centred at 480N and 120N correspond to the weakly pyritiferous feldspar porphyry. At 210S, anomaly G does not extend to depth but is surrounded by a larger zone of sub-anomalous chargeabilities. Thick peat at the surface here precludes any comparison with sub-outcropping geology.

Line 00

This profile has chargeability values mildly above background with several anomalous highs at depth (Fig. A3.2). A shallow (n=2) zone of low chargeabilities extends between 660N and 510N and this corresponds at the surface with quartzites. To each side of this low, sub-anomalous chargeability highs possibly extending to depth are centred at 690N and 420N which correspond with quartz-biotite schist/epidiorite boundaries. The resistivity low and chargeability high below 300N correspond with the position of the main fault where abundant sulphides have been recorded in adjacent epidiorite. The shallow, extensive zone of low to background chargeability extending southwards from 360N is associated with epidiorite and the weakly pyritiferous porphyry south of the main fault. The gap in the magnetic profile about 00 was caused by the steep magnetic gradient over a raft of epidiorite preventing measurements from being obtained.

Line 200W

This profile is highly anomalous north of the main fault and less so south of it (Fig. A3.3). The possibility that several sources (that have not been individually resolved by the dipoles) are contributing to the extensive anomalous chargeability zone between 600N and 120N is suggested by the 3 distinct magnetic anomalies centred at 540N, 330N and 180N. At the surface, these 3 anomalies occur along strike from 3 nearby exposed epidiorites of which the occurrence at 180N has locally common to abundant sulphides. It is suggested here, however, that two of the chargeability anomalies (centred at 510N 'D' and 360N), may be related as components of a larger chargeability pattern. This pattern is characterised by a central core at depth below 480N of background value chargeabilities, denoted (-), that is flanked each side by high value limbs which extend to depth (+). A similar

though less well defined pattern is discernible in the corresponding resistivity values, with highs and lows interchanged. When compared with those expected from IP models (Hauck, 1970, Coggan 1973, pp 742, 745), contour pattern suggests a 'slab-like' band of mineralisation occurring between the two (+) limbs at about 60 m depth with an apparent strike from east to west. (Here, 'slab-like' should be considered as being of a matchbox shape with face horizontal). Furthermore, the asymmetry of the observed contour pattern suggests the source may dip or become more tenuous to the south. Inspection of the lateral extent of the shallow (n=2) anomalous chargeability values and a comparison with IP models suggests that the source extends from 600N to 420N, possibly 300N. The negative and positive magnetic anomalies over 540N and 330N could then represent the northern and southern contacts of the body respectively, thereby suggesting the two epidiorites partially exposed beneath 540N and 330N are very close or even contiguous beneath thick peat. The chargeability anomaly at 180N is seen to be connected at depth to another anomaly below 30N which together cut off abruptly toward the east, where there is an associated resistivity low. At the surface this low corresponds with the main fault which probably dips to the north-west. Chargeability anomaly E at 270S and the anomaly at depth below 420S display a similar relationship. In particular both pairs of anomalies have similar trends to the south and have associated resistivity lows which at the surface are associated with nearby faults.

Line 400W

This line has mildly anomalous chargeabilities north of the main fault and low to background values south of it (Fig. A3.4). Centred at 540N, the sub-anomalous chargeability high corresponds at the surface to an exposure of epidiorite. The largest anomaly occurs at depth and may be related with

a broad negative magnetic anomaly at 330N. This anomaly occurs over an area mapped as quartzite that is tucked between two exposures of biotite-feldspar porphyry. The absence of anomalous values nearer the surface in this area, however, suggests a deeper source than the surface quartzite and may relate to an easterly extension along strike of the epidiorite nearby to the west. The high amplitude narrow negative magnetic anomaly at 150N and coincident shallow chargeability high are readily attributable to a raft of epidiorite in which abundant sulphides have been observed. This high is connected at depth to another local chargeability high below 60N. At the surface, these locations correspond with the main biotite-feldspar porphyry and are traversed by a possible fault at 50N. The sub-anomalous chargeability highs at 90S and at depth below 210S are connected and probably related to a shallow resistivity low and magnetic anomaly of the main fault and/or Tertiary dyke at 150S. The zone of low resistivity centred at 390S is probably related to the stream, wire fence and nearby fault which are coincident here.

Line 600W

This line which crosses the biotite-feldspar porphyry body along its western margin displays the largest anomalies encountered during the survey (Fig. A3.5). The presence of at least 3 anomalous magnetic sources is evident and these are observed to coincide with chargeability and/or resistivity anomalies. The most prominent of these magnetic anomalies coincides with the largest chargeability anomaly, labelled A. This anomaly and associated resistivity pattern is believed to be a component of a larger chargeability contour pattern of the type described previously in discussing the results of line 200W. This pattern suggests a shallow (about 60 m deep), thin 'slab-like' body, which, from inspection of the chargeability

plan contours for n=2 (Fig. 9), strikes from north-east to south-west. The horizontal extent of the shallow anomalous chargeability values suggests the anomalous source extends from 300N to 480N, which in the north corresponds to a fault (possibly two faults) intersecting this line. At 180N, a further zone, labelled 'A', has a prominent magnetic anomaly and also a sub-anomalous chargeability high that merges at depth with anomaly A. The contact zone between the main porphyry body and the above mentioned hornfels which is here traversed by a fault is thought to be a likely source for these anomalies. The southward continuation of the magnetic anomalies over the main porphyry body is probably due to granular magnetite which has been identified in the porphyry in this area. At approximately 360S, the high chargeability level is cut off where the main fault intersects this line. In this locality an extensive epidiorite is separated from the main fault-zone to the south by a small wedge of metasediments carrying massive sulphides in thin bands of quartzite. However, the chargeability contour pattern associated with anomaly C suggests a broad anomalous source in the form of a shallow (60 m deep), thin 'slab-like' body stretching north from 350S to at most 180S. Furthermore, the continuation of this anomaly to the north-east (as evident from the chargeability contours (Fig. 9)) suggests that the source may continue some distance under or within the main biotite-feldspar porphyry body. This suggests that the massive sulphides recognised within the wedge of metasediments near the fault may continue both north and north-eastwards within the epidiorite and possibly under the margins of the main biotite feldspar porphyry body.

Line 800W

This line passes some one hundred metres west of the main biotite-feldspar porphyry and displays prominent magnetic and chargeability anomalies (Fig. A3.6). Anomaly A, centred at 270N, is associated with a broader chargeability contour pattern discussed above. A similar pattern is discernible for the apparent resistivity values. This pattern suggests a shallow (60 m deep), thin 'slab-like' body and represents the south-west continuation of the anomalous zone crossing line 600W. The lateral extent of the shallow (n=2) anomalous chargeability values also suggests that the anomalous zone has a near surface width of about 180 m, extending north from about 180N and becoming more tenuous in the north. This anomaly coincides with the mapped continuation of the sulphide rich epidiorite traversed previously to the north-east on line 600W. Along strike to the south-west, recent mapping has recorded abundant sulphide, chiefly chalcopyrite and pyrite, within pebbly quartzite close to the southern contact of this epidiorite. Anomaly B, extending between 60N and 180S, has associated magnetic anomalies which correspond at the surface with two closely occurring epidiorites. These epidiorites strike from south-west to north-east and have probably been subjected to thermal alteration. Recent mapping has shown sulphides to occur over their exposed surface. The broad 'slab-like' source suggested by the contours for the source of these anomalies indicates that the epidiorites are contiguous or have failed to be resolved. Between anomalies A and B a shallow zone of high resistivity and lower chargeabilities occur and corresponds at the surface with quartzite.

The lateral extent northwards of the shallow anomalous values related to anomaly C suggests an extension, beneath overlying peat, of the epidiorite centred at 450S. This anomaly represents a south-westward continuation

along strike of the anomaly C on line 600W, where massive sulphides are in narrow horizons in metasediments. The more tenuous nature southwards of the chargeability anomaly associated with the epidiorite suggests that sulphides have been less well developed throughout. The string of positive magnetic anomalies straddling this epidiorite and the main fault, crossing at approximately 540S, are believed to be due to a combination of epidiorite to the north and/or pyrrhotite developed in quartzites to the south of the fault.

Line 1000W

This line is intersected by a nearby, long, north-south trending fault which is believed to have controlled to a large extent the distribution and nature of the anomalies (Fig. A3.7). The chargeability anomaly centred at 150N, which represents an apparent south-westerly termination to the elongate anomaly A, is here seen to have no associated magnetic anomaly, in contrast with lines 600W and 800W. Furthermore, the lateral extent of the shallow anomalous chargeability values corresponds at the surface to quartzite. In view of the very close proximity of the fault to the east, it is suggested that any original continuation south-westwards from the fault of the source of anomaly A has been cut out by the fault. The anomaly at 150N, therefore, is suggested as representing the side effects of the nearby anomalous zone immediately east of the fault. Immediately north of the fault intersection near 90S, the large positive magnetic anomaly over 30N corresponds with epidiorite. South of the baseline, the fault is virtually coincident with line 1000W, a fact which is apparently indicated by the extensive zone of low resistivity between 00 and 360S. The zone of mildly anomalous chargeabilities between 90S and 240S seem to be related to two occurrences of epidiorite but may also be related in part to graphite or sulphides including pyrrhotite developed along the fault plane. South of

300S, chargeability values fall to below background level suggesting that sulphides are poorly developed. At the surface this area contains thick peat with local exposures of quartzite and epidiorite. Coincident with these low chargeabilities is a zone of strong magnetic anomalies which, in the absence of epidiorite, suggests that pyrrhotite occurs in the quartzite but not in sufficient quantity as to increase chargeability values. Alternatively, more epidiorite that is low in sulphides but containing magnetite say, may underlie the peat cover than is suggested by the geological map.

Line 420N

The chargeability contour pattern for this profile is characterised by at least 2 strongly anomalous zones A and D, while 2 other sub-anomalous zones are recognisable near the ends of this line (Fig. A3.8). These patterns have been discussed above for other lines and are indicative of shallow, thin, 'slab-like' zones of mineralisation. Anomaly A has previously been associated with a 'highly pyritiferous hornfels'. It is, however, noteworthy that the interpreted source of anomaly A is bounded by two sub-parallel north-south trending faults. This is regarded as important since it suggests that the process or processes responsible for developing pyritic zones within epidiorite nearby have also been effective here but have subsequently been cut off in the east and west by later faulting. Anomaly D, while well resolved in the west, is disturbed by a neighbouring sub-anomalous zone to the east, which suggests the associated surface epidiorites, which are centred at 250W and 50W, are less than 60 m apart beneath the overlying peat cover. This conclusion has previously been arrived at in discussing this anomaly on line 200W.

Baseline

This line passes across the centre of the main biotite-feldspar porphyry body and is anomalous to the west of a north-south trending fault which intersects the western margin of this porphyry near 720W (Fig. A3.9). This fault is indicated by the resistivity low, abrupt fall off in chargeability values and negative magnetic anomaly. West of the fault, chargeability anomaly B and positive magnetic anomalies are associated at the surface with two exposures of epidiorite which have not been resolved separately. Pyrrhotite in quartzite may also, however, be a source for the magnetic anomalies. The chargeability anomaly at depth below 690W is related to the shallower anomaly B which together display a pattern similar to chargeability anomalies associated with faults (see for example line 200W). The continuation of this anomaly at depth to the east below the biotite-feldspar porphyry body, and the related similar extension northwards at depth of anomaly C on line 600W, may indicate the base of the central zone of non-biotitic, weakly mineralised porphyry of the main Garbh Achadh intrusion. East of the fault, over the main biotite-feldspar porphyry body, shallow chargeability values are low and the magnetic field values fall away to background. The main fault which crosses this line near 240W is clearly indicated by a resistivity low. East of this fault, shallow low chargeability values correspond at the surface with epidiorite and weakly pyritiferous porphyry which may have limited depth extent in view of the higher chargeabilities at depth.

Line 420S

Although not as well defined as elsewhere, a chargeability contour pattern suggesting a 'slab-like' source has been recognised as centred over 760W which is associated with anomaly C (Fig. A3.10). The lateral

extent of this zone is found to correspond with a thermally altered epidiorite which nearby is known to contain sulphides. The eastern boundary to this anomaly corresponds with the main fault crossing near 700W. East of this fault, chargeability values are low. A further fault is recognised by the resistivity low at 490W. Lack of detailed geological control has precluded any correlation with the shallow anomaly F at the end of this line.

Line 600W (120 m dipoles)

In view of the magnitude and continuation at depth of the large IP anomaly A, this line was further investigated using a larger dipole length in order to ascertain whether it widened significantly at depth. Inspection of Fig. A3.11 shows that although the individual anomalies are no longer so well defined, the extensive chargeability patterns associated with anomalies A and C are still evident, but anomalies A and A' have no longer been resolved separately. Qualitatively it may be argued that had the anomalous body become significantly wider at depth, then the observed IP effects would not vary greatly with the increased dipole lengths and separations. This is not observed, since the measured IP effects decrease when the 120 m dipoles are used. It is inferred, therefore, that in the larger volume of earth sampled using the 120 metre dipoles, the anomalous body has less effect. It follows that the sources of the anomalous zones A and C neither widen nor continue significantly at depth.